

Special Topics in Particle Physics

Particle and Radiation Detection

Helga Dénés 2024 S1 Yachay Tech

hdenes@yachaytech.edu.ec

Particle and radiation detection

The measurement techniques relevant to astroparticle physics are very diverse and the detection of astroparticles is usually a multistep process.

Particle detection is mostly indirect. It is important to identify the nature of the astroparticle in a suitable interaction process. The target for interactions is, in many cases, not identical with the detector that measures the interaction products.

Cosmic-ray muon neutrinos, for example, interact via *neutrino–nucleon interactions in the antarctic ice or in the ocean, subsequently producing charged muons*. These muons suffer energy losses from electromagnetic *interactions in the ice (water)*, in which, among others, *Cherenkov radiation* is produced. The Cherenkov light is recorded, via the photoelectric effect, by *photomultipliers*. This is then used to **reconstruct the energy and the direction of incidence of the muon**, which is **approximately identical to the direction of incidence of the primary neutrino**.

Particle and radiation detection

The **cross sections** for the various processes depend on the **particle nature, the particle energy, and the target material**. A useful relation to determine the **interaction probability** ϕ and the event rate is obtained from the atomic-(σ_A) or nuclear-interaction cross section (σ_N) according to

$$\phi \{(\text{g}/\text{cm}^2)^{-1}\} = \frac{N_A}{A} \sigma_A = N_A \{\text{g}^{-1}\} \sigma_N \{\text{cm}^2\}$$

where N_A is Avogadro's number, A is the atomic mass of the target, and σ_A is the atomic cross section in cm^2/atom (σ_N in $\text{cm}^2/\text{nucleon}$). If the target represents an area density $d \{\text{g}/\text{cm}^2\}$ and if the flux of primary particles is $F \{\text{s}^{-1}\}$, the **event rate** R is obtained as

$$R = \phi \{(\text{g}/\text{cm}^2)^{-1}\} d \{(\text{g}/\text{cm}^2)\} F \{(\text{s}^{-1})\}.$$

$$\phi \{(\text{g}/\text{cm}^2)^{-1}\} = \frac{\mu}{\varrho} = \frac{N_A}{A} \sigma_A$$

$$\phi \{(\text{g}/\text{cm}^2)^{-1}\} = \sigma_N N_A.$$

Interactions of Astroparticles

The primary particles carrying astrophysical information are:

- nuclei (protons, helium nuclei, iron nuclei, etc.),
- electrons,
- photons,
- neutrinos.

These categories of particles are characterized by **completely different interactions**.

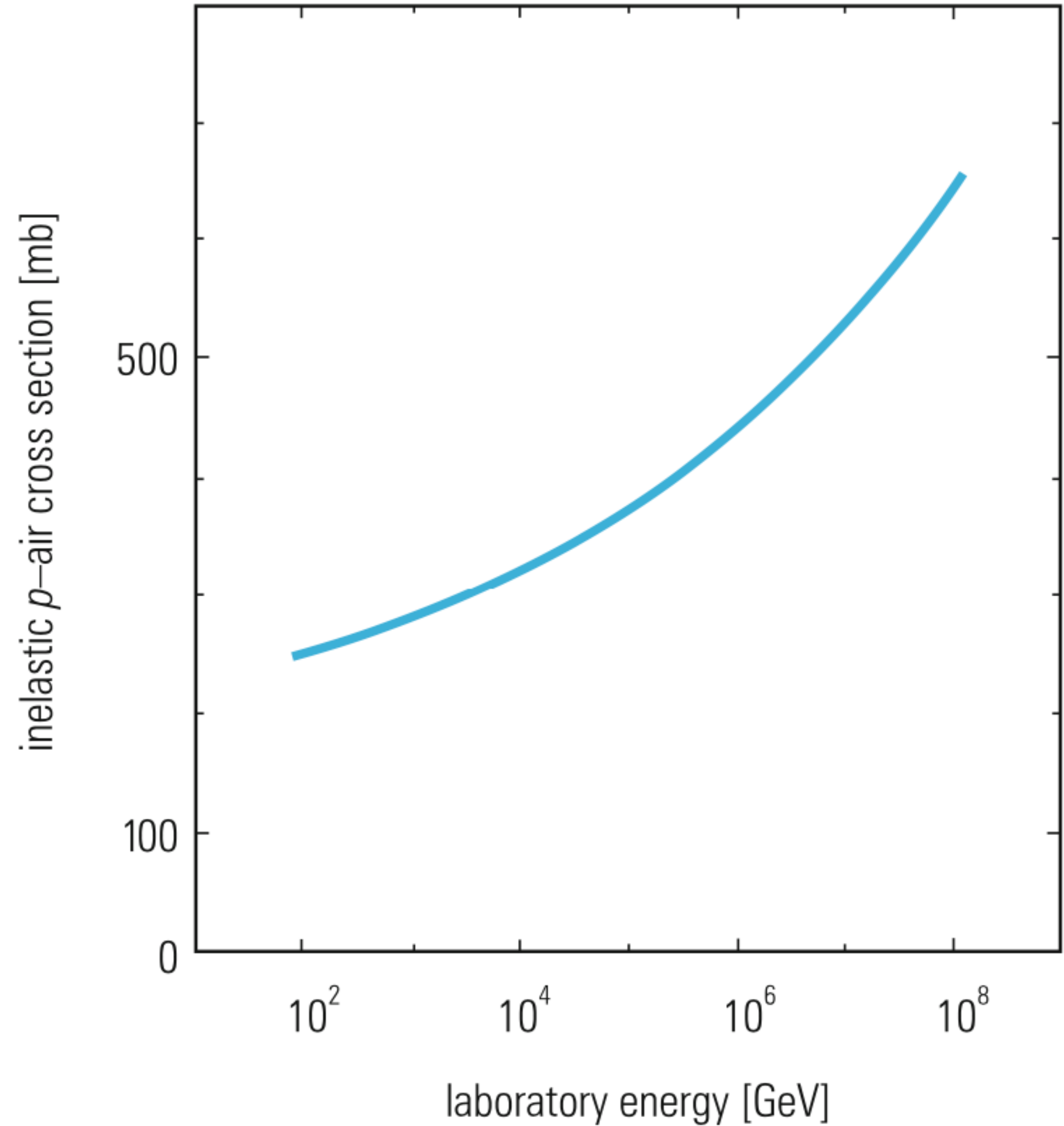
Protons and other nuclei will undergo strong interactions. They are also subject to electromagnetic and weak interactions, however, the corresponding cross sections are much smaller than those of strong interactions.

Primary nuclei will therefore interact predominantly via processes of strong interactions.

Interactions of Astroparticles

Fig. 4.1 Cross section for proton–air interactions

A typical interaction cross section for inelastic proton–proton scattering at energies of around 100 GeV is $\sigma_N \approx 40 \text{ mb}$ ($1\text{mb} = 10^{-27} \text{ cm}^2$). Since high-energy primary protons interact in the atmosphere via **proton–air interactions**, the cross section for proton–air collisions is of great interest. The dependence of this cross section on the proton energy is shown in Fig. 4.1.



Interactions of Astroparticles

For a typical interaction cross section of 250 mb, the *mean free path* of protons in the atmosphere (for nitrogen: $A = 14$) is, see Chap. 3, (3.6.2),

$$\lambda = \frac{A}{N_A \sigma_A} \approx 93 \text{ g/cm}^2.$$

The interaction length for hadrons (protons, pions, ...) is defined through this, where σ_A is the total cross section. This length is sometimes also called **collision length**. If the total cross section is replaced by its inelastic part only, the resulting length is called *absorption length*.

This means that the **first interaction of protons occurs in the upper part of the atmosphere**.

If the primary particles are not protons but rather iron nuclei (atomic number $A_{\text{Fe}} = 56$), the first interaction will occur at even higher altitudes because the **cross section for iron–air interactions is correspondingly larger**.

$$\lambda \{\text{cm}\} = \frac{A}{N_A \{\text{g}^{-1}\} \varrho \{\text{g/cm}^3\} \sigma_A \{\text{cm}^2\}}$$

Interactions of Astroparticles

Primary high-energy photons (energy $\gg 10$ MeV) interact via the **electromagnetic process of electron–positron pair production**. The characteristic interaction length ('radiation length') for electrons in air is $X_0 \approx 36$ g/cm².

For high-energy photons (energy ≥ 10 GeV), where pair production dominates, the cross section is 7/9 of the cross section for electrons, so the radiation length for photons is 9/7 of that for electrons, i.e., 47 g/cm². The first interaction of **photon-induced electromagnetic cascades therefore also occurs in the uppermost layers of the atmosphere**.

The radiation length for electrons is defined in (4.2.2). It describes the degrading of the electron energy by bremsstrahlung according to $E = E_0 e^{-x/X_0}$. This 'interaction length' X_0 is also characteristic for pair production by photons.

$$-\frac{dE}{dx} \Big|_{\text{brems}} = 4\alpha N_A \frac{Z^2}{A} r_e^2 E \ln \frac{183}{Z^{1/3}} = \frac{E}{X_0}, \quad (4.2.2)$$

Interactions of Astroparticles

The detection of cosmic-ray **neutrinos** is completely different. They are only subject to **weak interactions** (+gravity). The cross section for neutrino–nucleon interactions is given by

$$\sigma_{\nu N} = 0.7 \times 10^{-38} E_\nu [\text{GeV}] \text{ cm}^2/\text{nucleon}$$

Neutrinos of 100 GeV possess a tremendously large interaction length in the atmosphere:

$$\lambda \approx 2.4 \times 10^{12} \text{ g/cm}^2$$

This number has to be compared to the area density of the Earth of $7 \times 10^9 \text{ g/cm}^2$ for the passage through its center. The vertex for possible neutrino–air interactions in the atmosphere should consequently be uniformly distributed along the neutrino track in the atmosphere.

Charged and/or neutral particles are created in the interactions, independent of the identity of the primary particle. These **secondary particles** will, in general, be **recorded by the experiments or telescopes**. To achieve this, a large variety of secondary processes can be used.

Interactions used for particle detection

Figures 4.2 and 4.3 show the main interaction processes of charged particles and photons, as they are typically used in experiments in astroparticle physics. In this overview, not only the interaction processes are listed, but also the typical detectors that utilise the corresponding interaction processes.

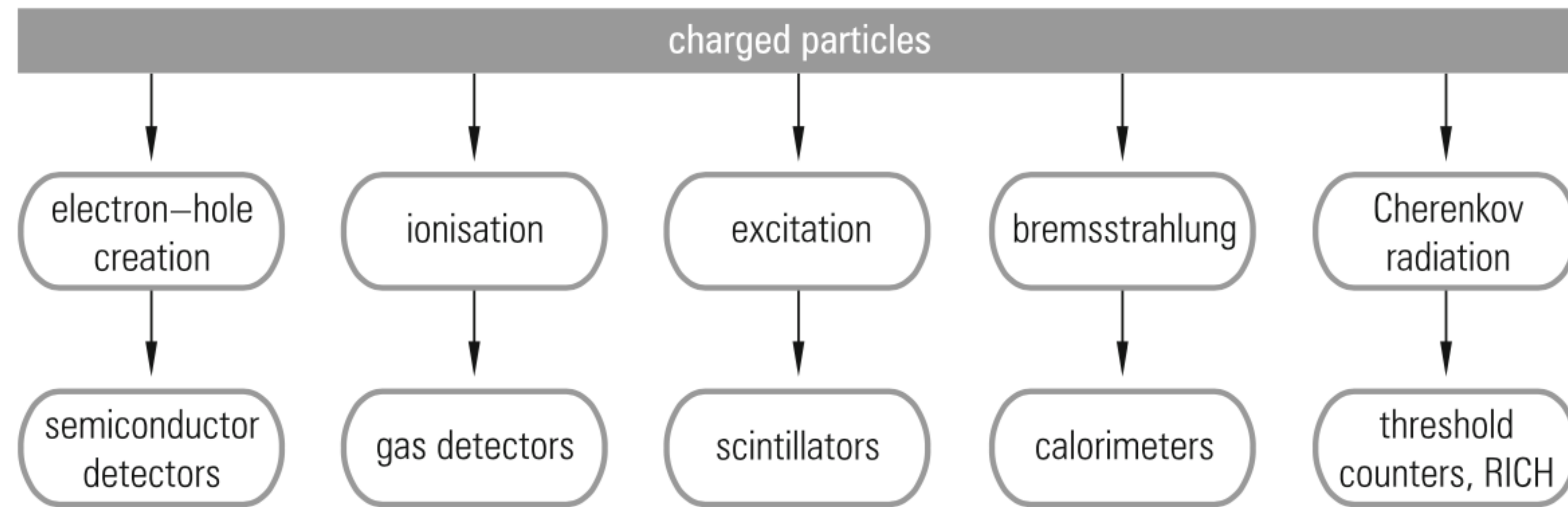


Fig. 4.2 Overview of interaction processes of charged particles

Interactions used for particle detection

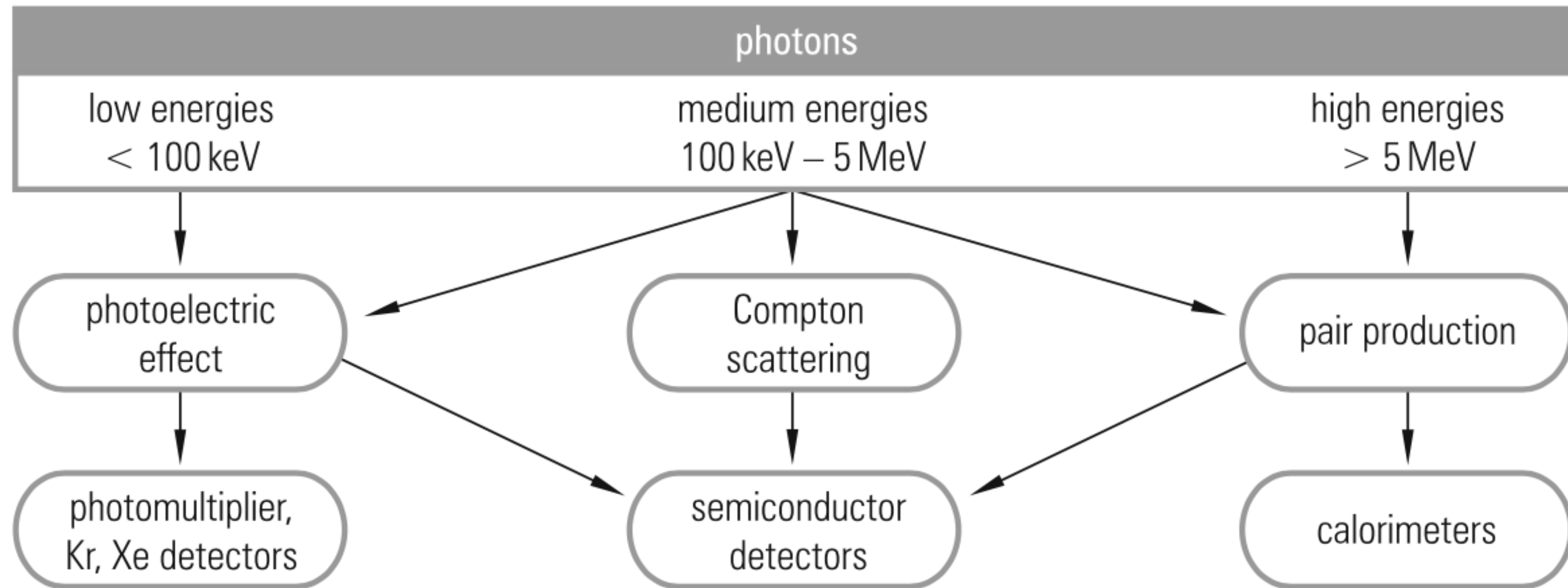


Fig. 4.3 Overview of interaction processes of photons

Interactions used for particle detection

The mechanism that dominates charged-particle interactions is the **energy loss by ionization and excitation**. This **energy-loss process is described by the Bethe–Bloch formula**:

$$-\frac{dE}{dx} \Big|_{\text{Ion.}} = K \cdot z^2 \frac{Z}{A} \cdot \frac{1}{\beta^2} \left\{ \frac{1}{2} \ln \frac{2m_e c^2 \beta^2 \gamma^2 T_{\max}}{I^2} - \beta^2 - \frac{\delta}{2} \right\}$$

$K = 4\pi N_A r_e^2 m_e c^2 = 0.307 \text{ MeV}/(\text{g/cm}^2)$;

N_A – Avogadro number;

r_e – classical electron radius ($= 2.82 \text{ fm}$);

$m_e c^2$ – electron rest energy ($= 511 \text{ keV}$);

z – projectile charge;

Z, A – target charge and target mass;

β – projectile velocity ($= v/c$);

$\gamma = 1/\sqrt{1 - \beta^2}$;

$T_{\max} = \frac{2m_e p^2}{m_0^2 + m_e^2 + 2m_e E/c^2}$,

maximum energy transfer to an electron,

m_0 —mass of the incident particle,

p, E —momentum and total energy of the projectile;

I – average ionization energy of the target;

δ – density correction.

Interactions used for particle detection

The energy loss of charged particles, according to the Bethe–Bloch relation, is illustrated in Fig. 4.4 and Fig. 4.5. It exhibits a $1/\beta^2$ increase at low energies.

The minimum ionization rate occurs at around $\beta\gamma \approx 3.5$. This feature is called the **minimum of ionization**, and particles with such $\beta\gamma$ values are said to be **minimum ionizing**.

For **high energies, the energy loss increases logarithmically ('relativistic rise')** and reaches a **plateau ('Fermi plateau')** owing to the density effect. The energy loss of gases in the plateau region is typically 60% higher compared to the ionization minimum.

The energy loss of singly charged minimum-ionizing particles by ionization and excitation in air is $1.8\text{MeV}/(\text{g/cm}^2)$ and $2.0\text{MeV}/(\text{g/cm}^2)$ in water (ice).

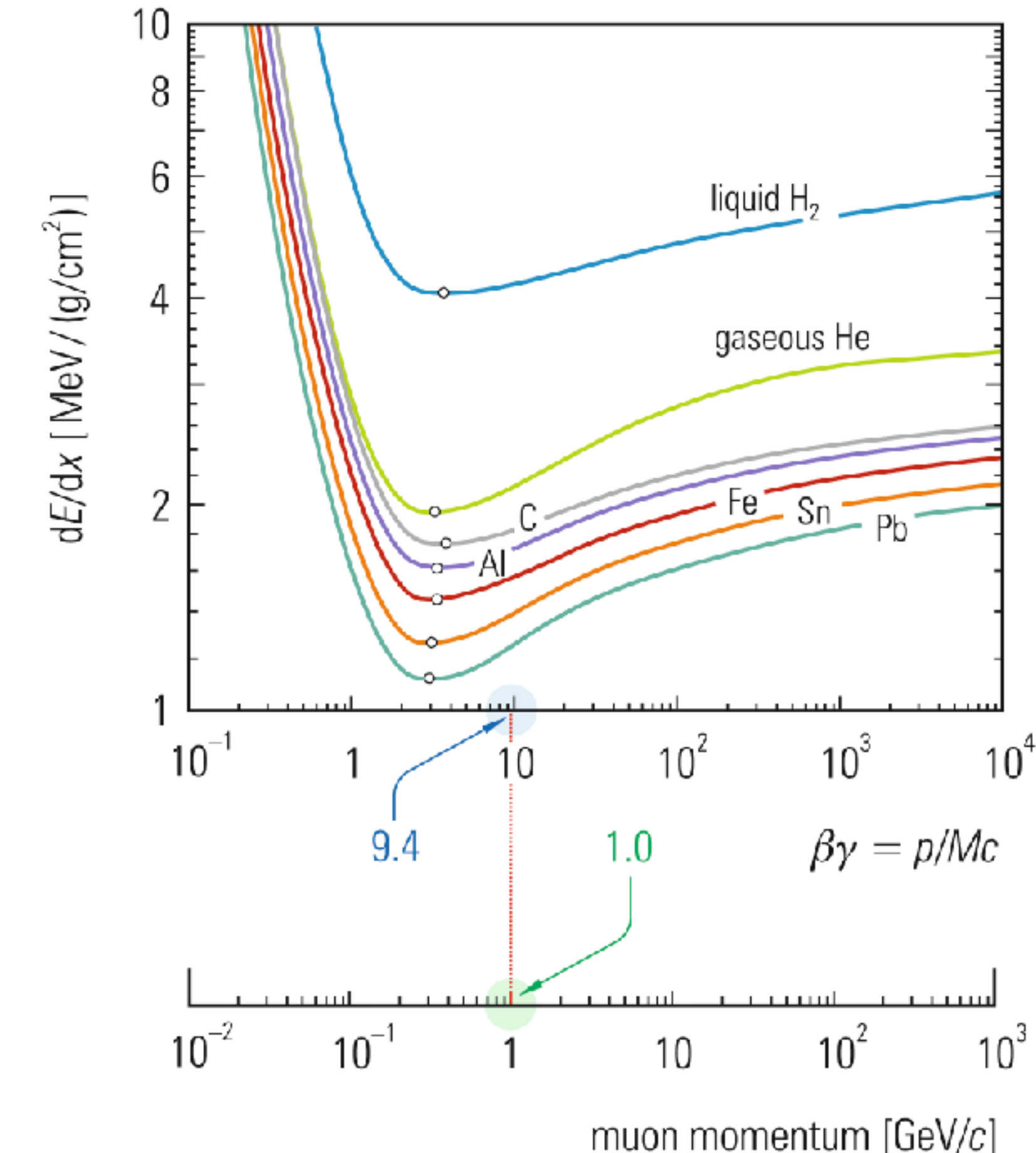


Fig. 4.4 Energy loss of charged particles in various targets. The curves are universal for all charged particles if the $\beta\gamma$ scale is used. The energy loss of different particles depends, of course, on their momenta, which are different for a particular particle type for a given $\beta\gamma$ value. For example, a muon of momentum of $1\text{ GeV}/c$ corresponds to $\beta\gamma = 9.4$. In general the momentum p is given by $p = M \cdot c \cdot \beta\gamma$

Interactions used for particle detection

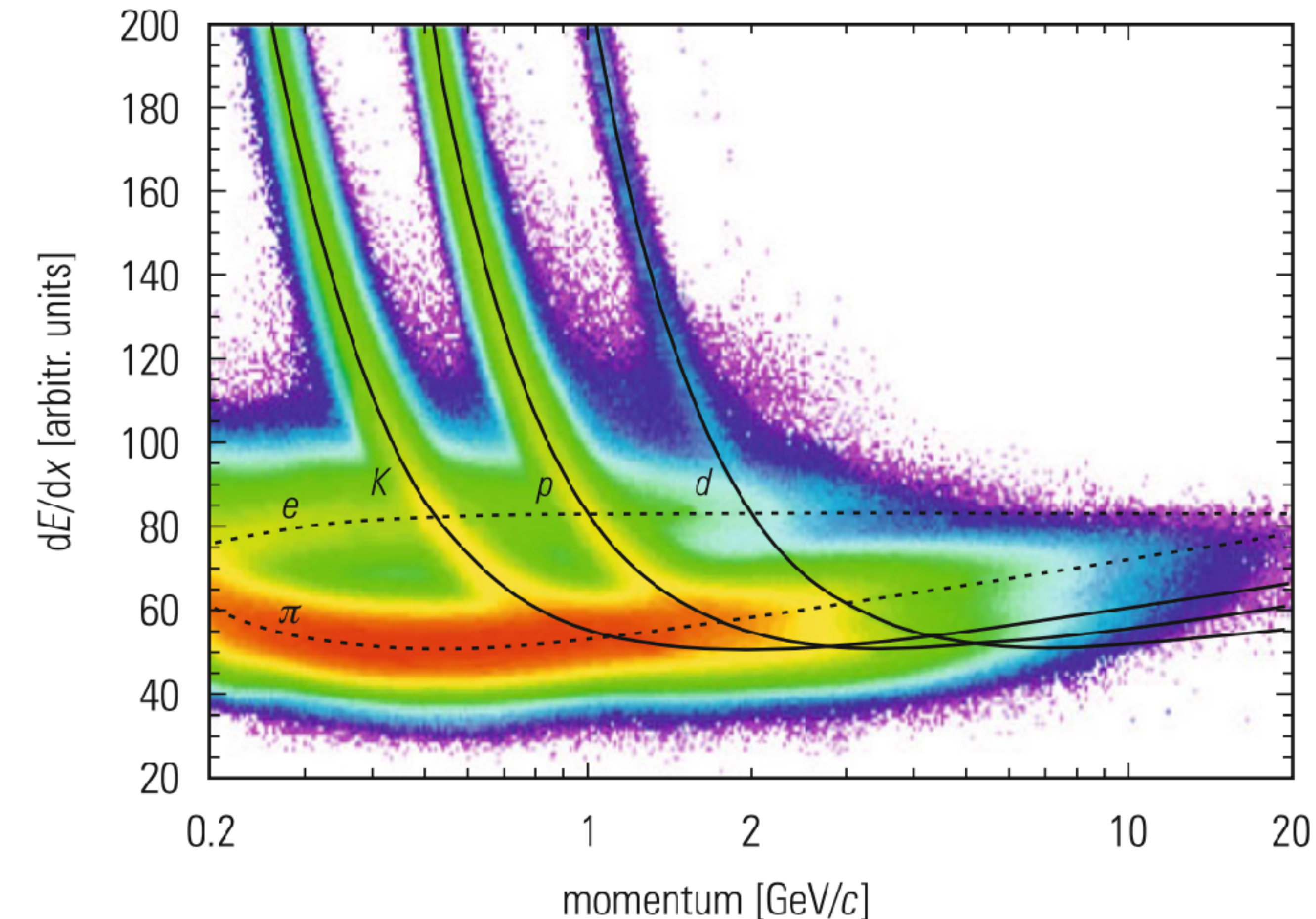


Fig. 4.5 Particle identification in the time projection chamber of the ALICE experiment at the LHC [33]

Interactions used for particle detection

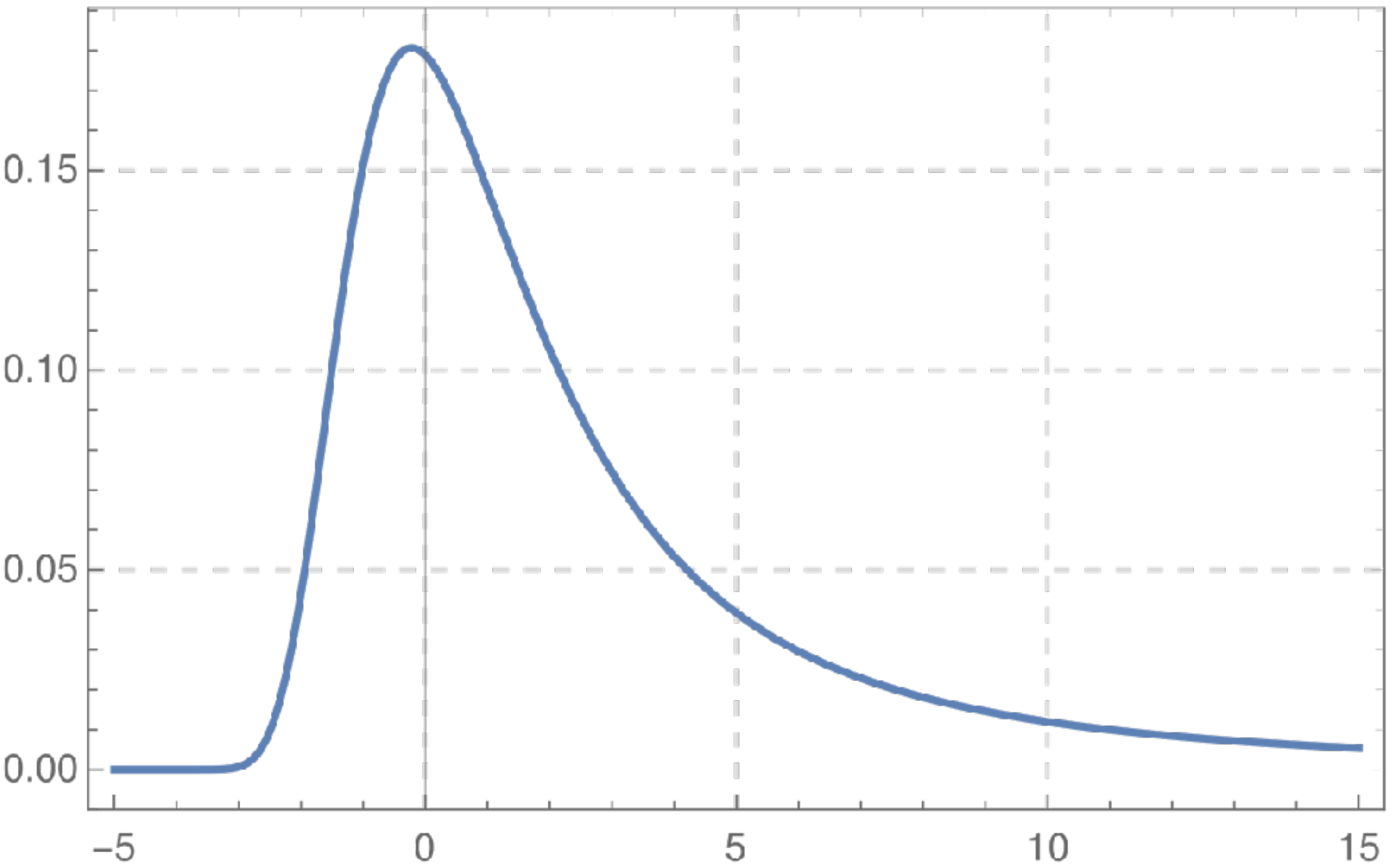
- For the production of an electron–positron pair in air an average energy of 30 eV is required.
- In contrast, in **semiconductor counters** the average energy for the creation of an electron–hole pair is **only 3 eV**.
- The average energy needed to produce a **scintillation photon in inorganic materials** (e.g., NaI) is about **25 eV** and **≈100 eV in organic materials**.
- **Semiconductor detectors can be made very small** and allow as pixel detectors **high spatial resolutions**. In astroparticle physics they are mainly used in **satellite experiments** or on the International Space Station (ISS).
- The Equation only **describes the average energy loss** of charged particles. The energy loss is **distributed around the most probable value** by an **asymmetric Landau distribution**. The **average energy loss** is **about twice as large as the most probable energy loss**. The ionization energy loss is the **basis of a large number of particle detectors**.

$$-\frac{dE}{dx} \Big|_{\text{Ion.}} = K \cdot z^2 \frac{Z}{A} \cdot \frac{1}{\beta^2} \left\{ \frac{1}{2} \ln \frac{2m_e c^2 \beta^2 \gamma^2 T_{\max}}{I^2} - \beta^2 - \frac{\delta}{2} \right\}$$

Landau distribution

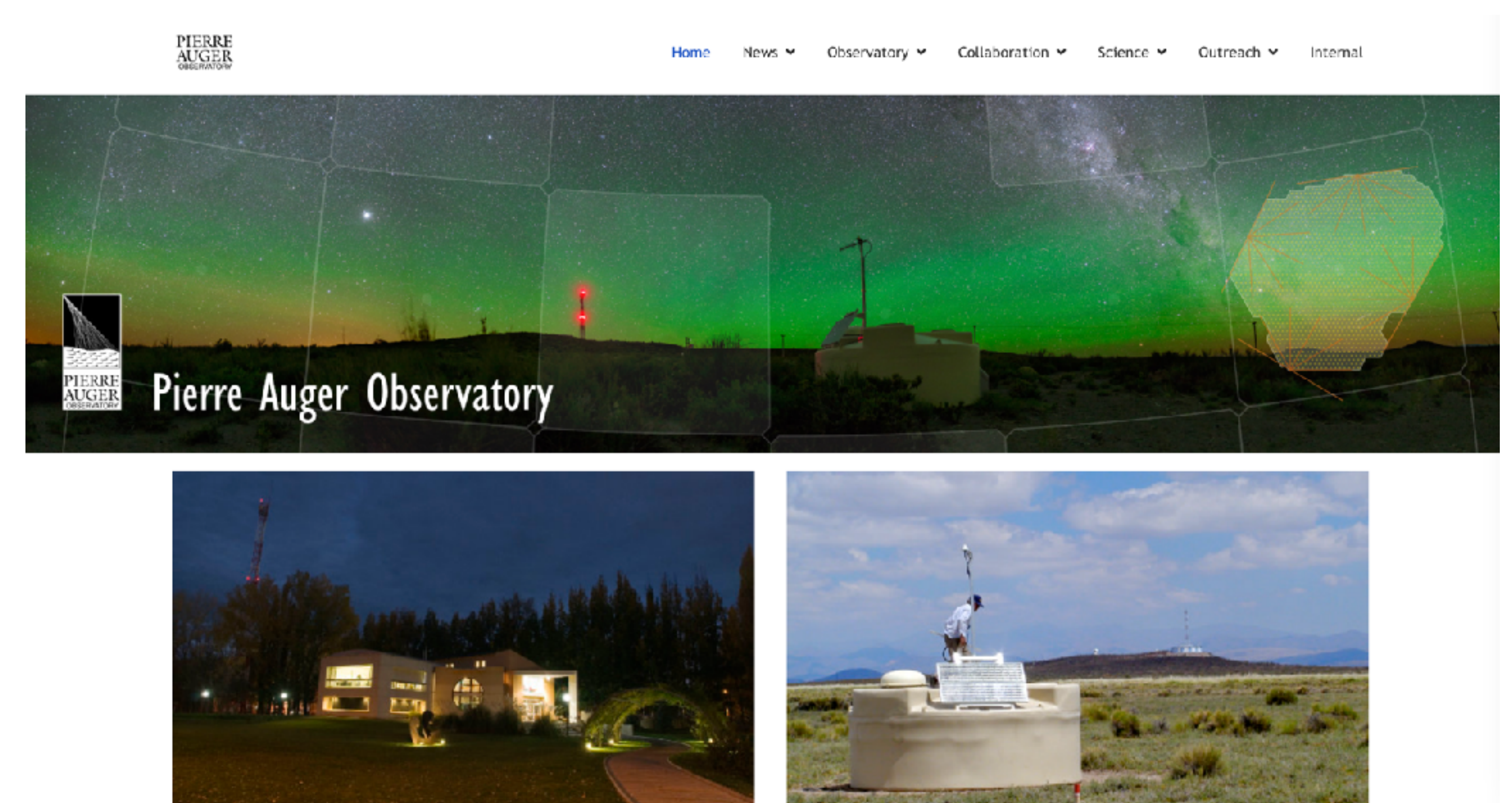
Probability distribution:

$$p(x) = \frac{1}{2\pi i} \int_{a-i\infty}^{a+i\infty} e^{s \log(s) + xs} ds,$$



Interactions used for particle detection

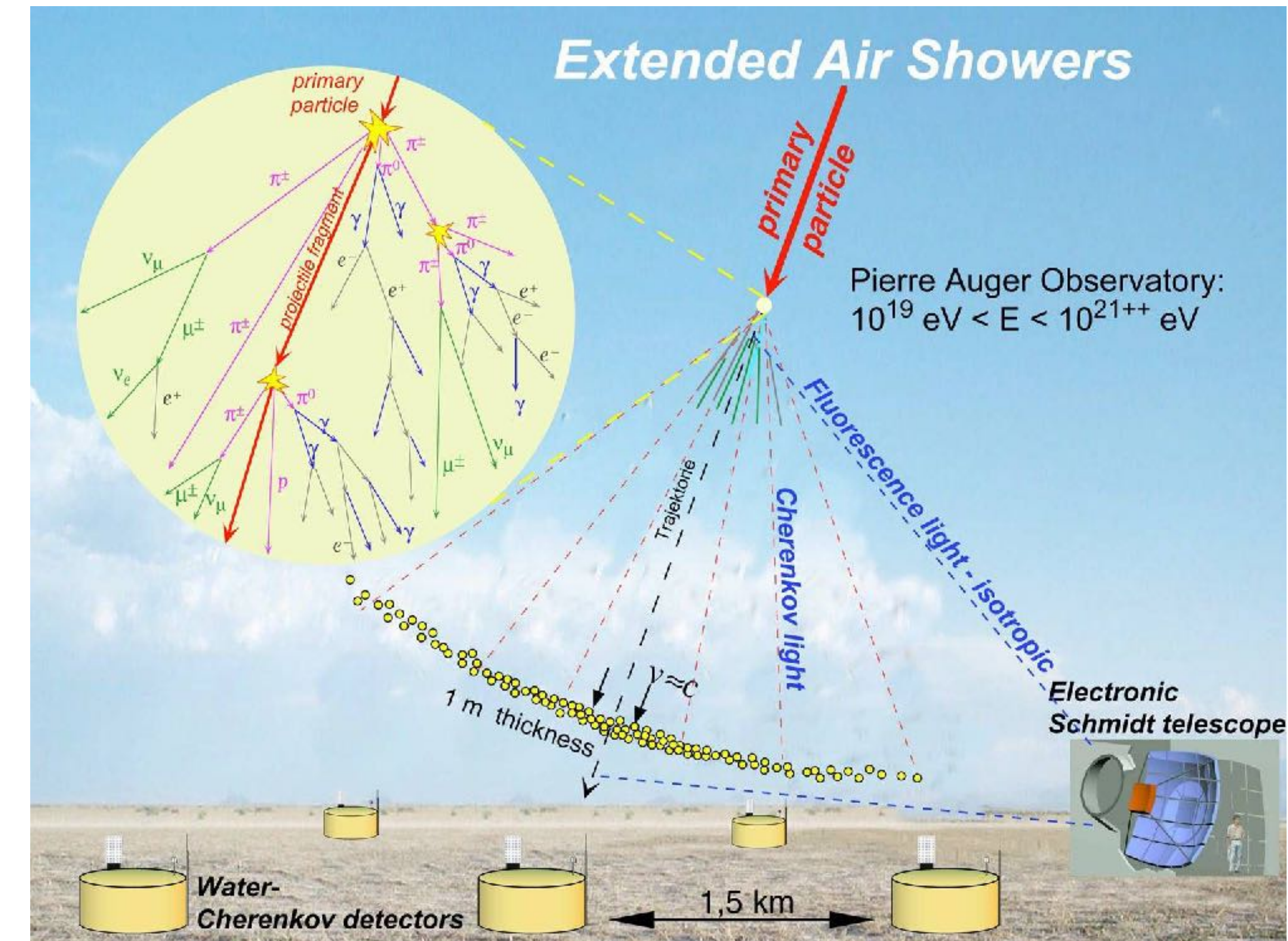
- The scintillation of gases is used in fluorescence telescopes for energies \geq EeV ($\geq 10^{18}$ eV, exa electron volt) in the field of particle astronomy, like in the **Auger experiment**.
- In these experiments the atmosphere represents the target for the primary particle. The **interaction products create scintillation light in the air**, which is recorded in telescopes on the ground equipped with photomultipliers mounted in the focal plane of mirrors.



Pier Auger Observatory (Argentina)

The acceleration of most low energy cosmic rays is related to various types of magnetic fields in space. These magnetic fields are known to exist on the sun, in the solar wind, and in the remnants of supernova explosions in our Milky Way Galaxy. Interactions of charged particles with these fields can account for cosmic rays with energies ranging from 10^9 eV to 10^{16} eV.

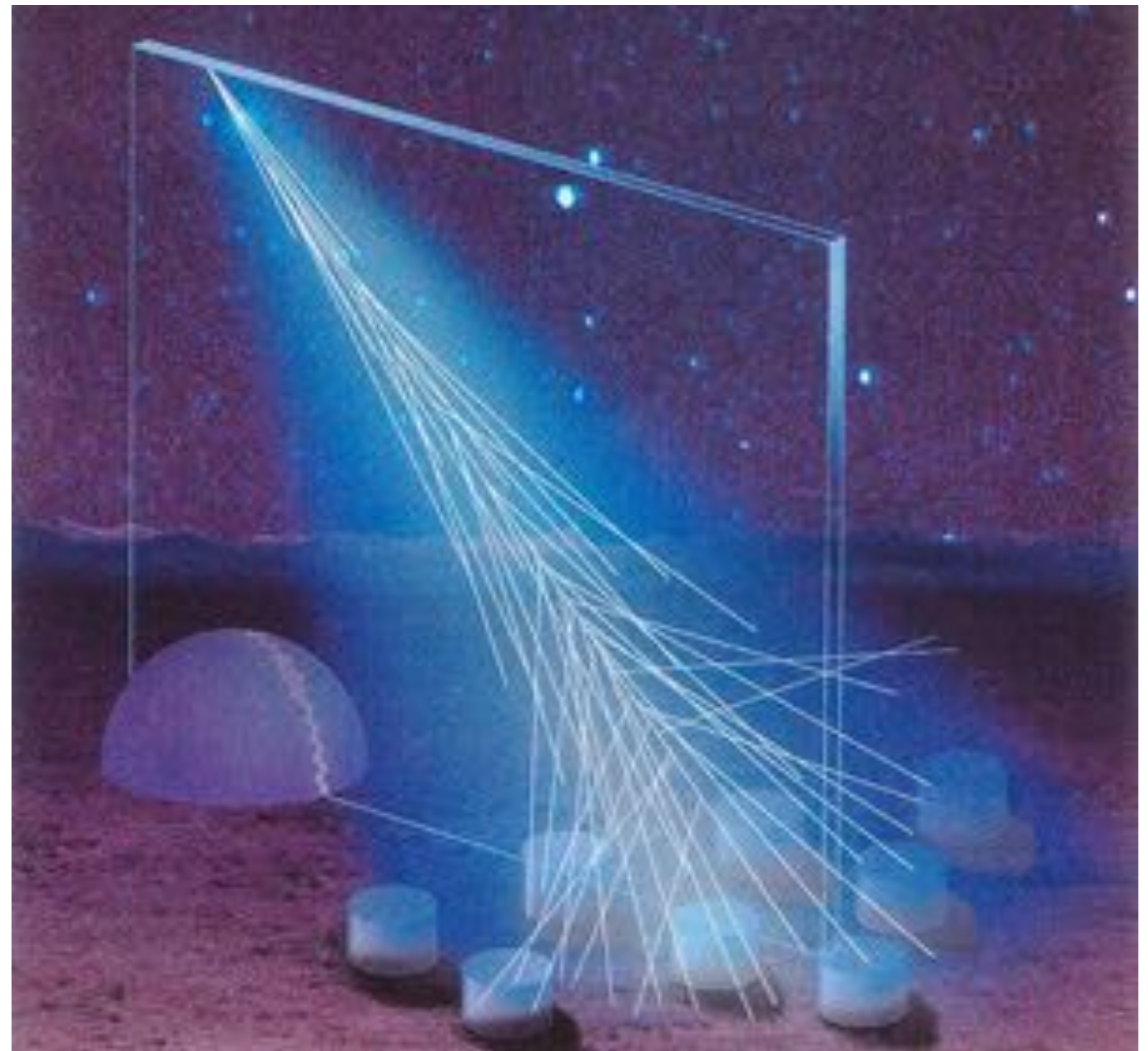
Occasionally, however, a cosmic ray with an **energy above 10^{19} eV** is detected. There is no scientific consensus on how or where cosmic rays with these ultra-high energies originate.



Pier Auger Observatory (Argentina)

The highest energy cosmic rays are **extremely rare**. Cosmic rays with energies above 10^{19} eV arrive on Earth **at a rate of only 1 particle per square kilometer per year**. The cosmic rays with energies of over 10^{20} eV, have an estimated arrival rate of just **1 per square kilometer per century!** In order to record a large number of these remarkable events, the Auger Observatory has created a detection area in western Argentina a bit larger than the country of Luxembourg.

The Auger Observatory is a "hybrid detector", employing two independent methods to detect and study high-energy cosmic rays. One technique detects high energy particles through their interaction with water placed in surface detector tanks. The other technique tracks the development of air showers by observing ultraviolet light emitted high in the Earth's atmosphere. The hybrid nature of the Pierre Auger Observatory provides for two independent ways to see cosmic rays.

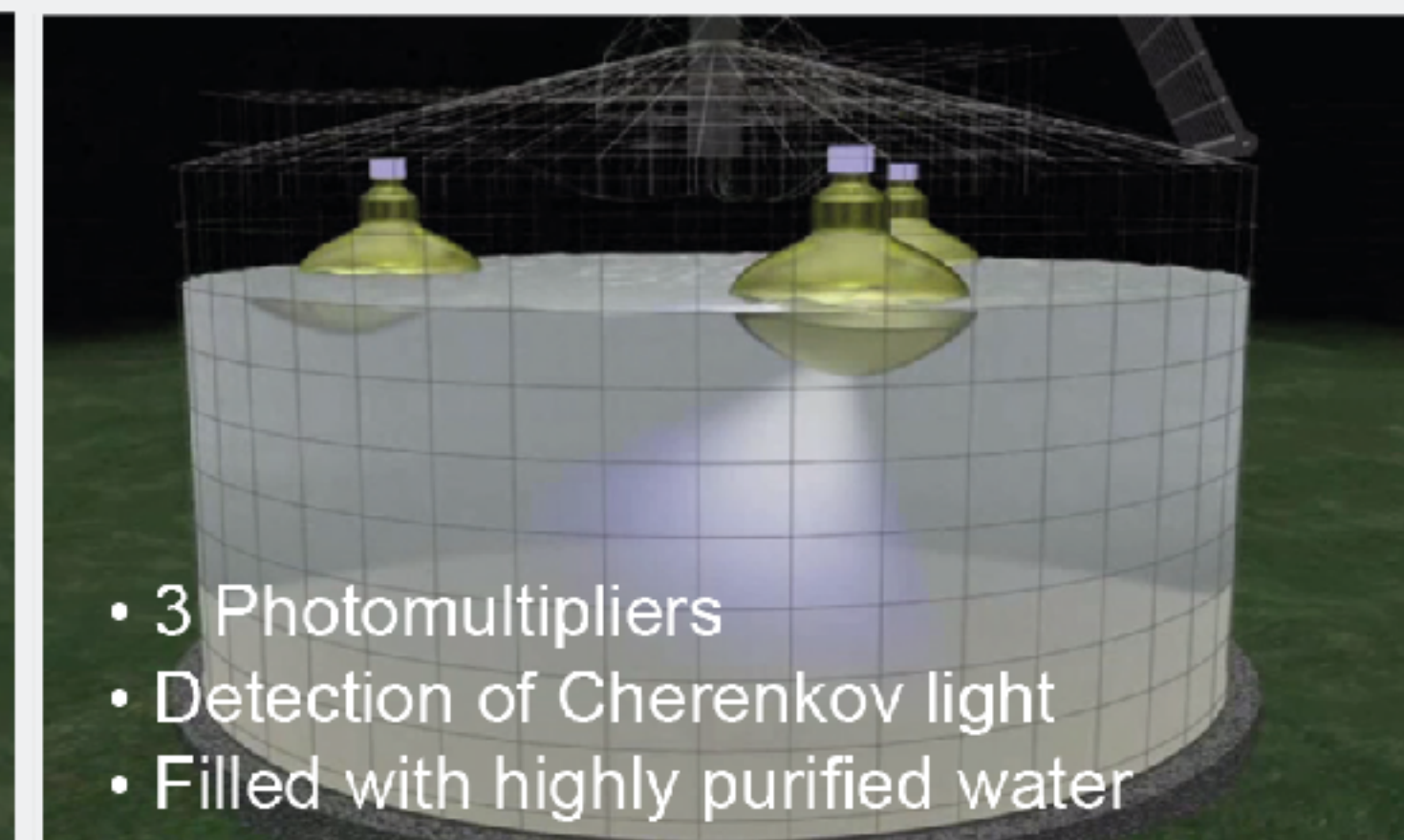
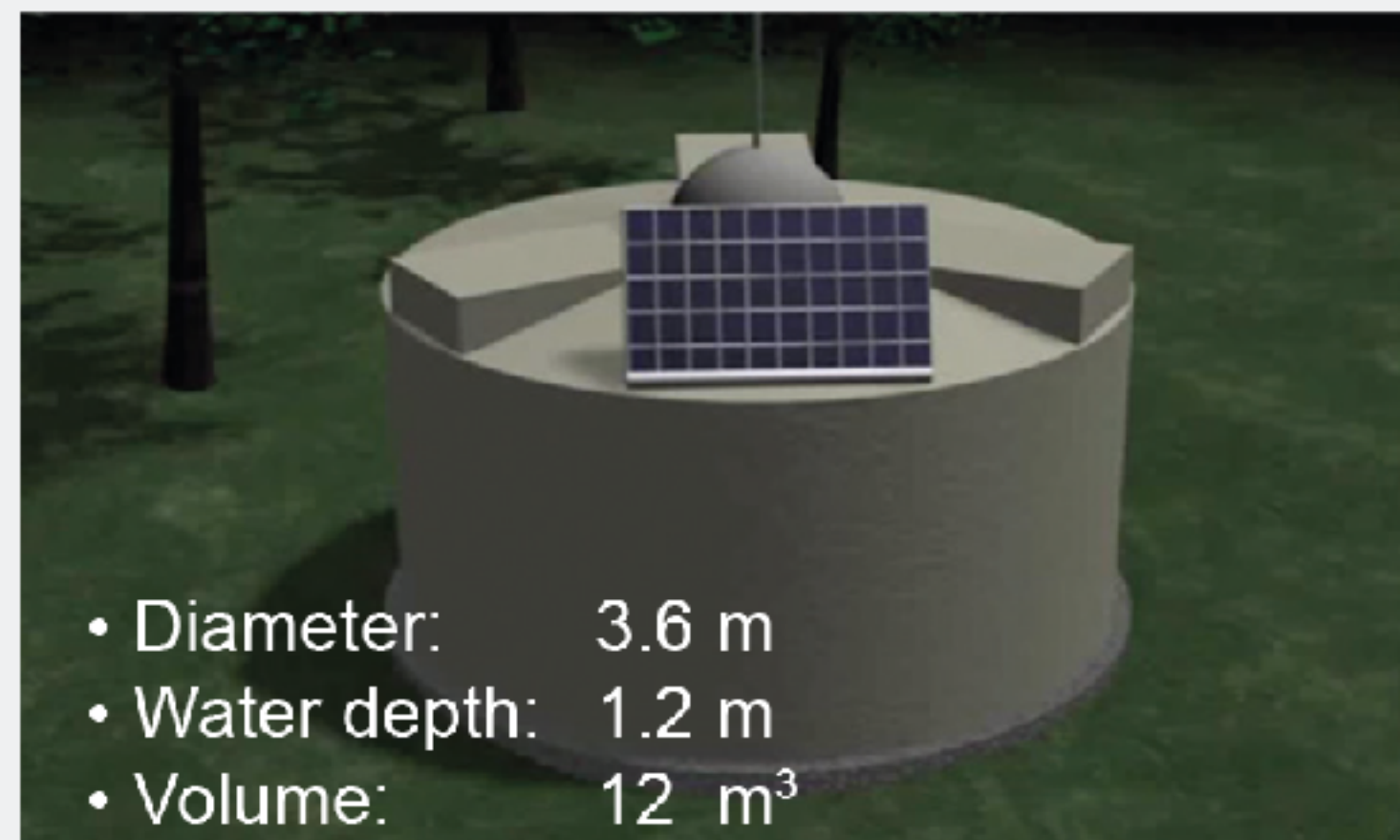


Pier Auger Observatory (Argentina)

The first detection method uses 1,660 water surface detector tanks that cover about 3,000 km² of the Pampa and serve as particle detectors. Each 12,000 liter tank, separated from each of its neighbors by 1.5 kilometers, is completely dark inside. Cosmic ray particles from particle showers produce **Cherenkov light** that can be measured by photomultiplier tubes mounted on the tanks. Extensive air showers contain billions of secondary particles and can cause **nearly simultaneous bursts of light in more than five tanks**. Scientists can **determine the energy of the primary cosmic ray particle based on the amount of light they detect from a sample of secondary particles**. Slight differences in the detection times at different tank positions help scientists determine the **trajectory** of the incoming cosmic ray.

Surface Detector

1,660 surface detector stations
(1,500 m apart from each other)

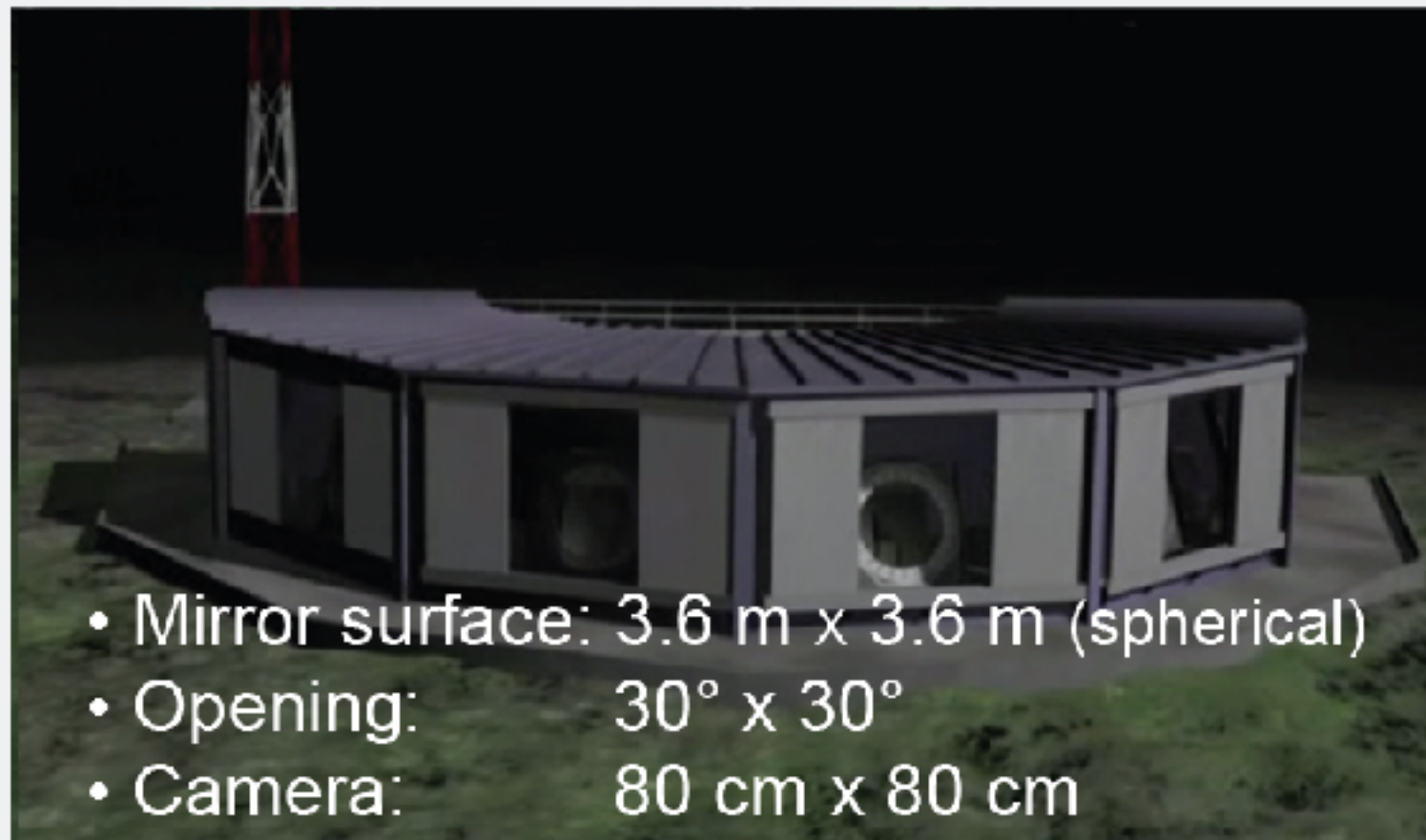


Pier Auger Observatory (Argentina)

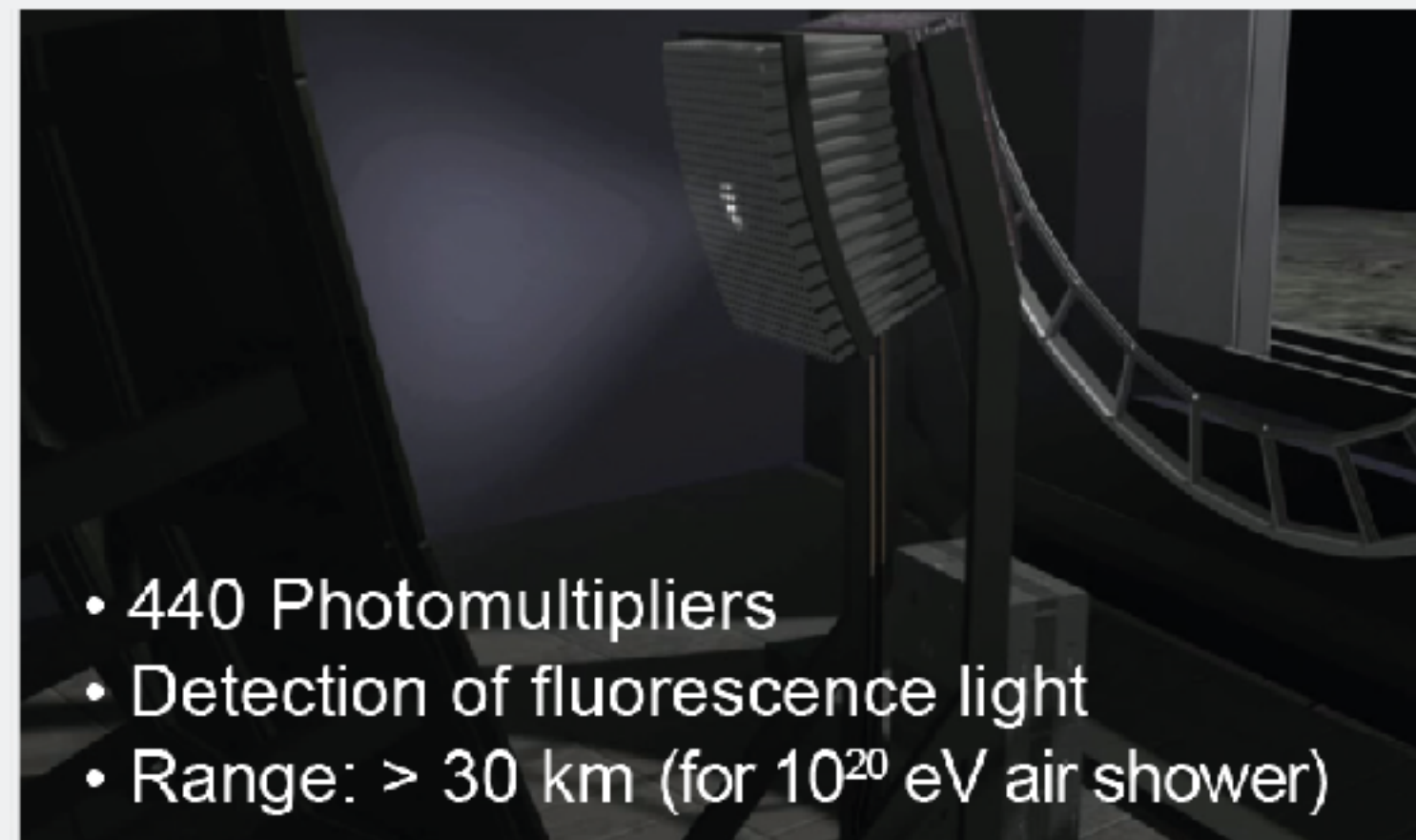
The charged particles in an air shower also **interact with atmospheric nitrogen, causing it to emit ultraviolet light via a process called fluorescence**. The observatory's second detection method uses these detectors to observe the trail of nitrogen fluorescence and track the development of air showers by measuring the brightness of the emitted light. To the fluorescence detectors, a cosmic ray looks like a UV light bulb rocketing through the atmosphere at the speed of light, with an ever-increasing brightness that **can reach up to four watts as the cascade grows to its maximum size**. Using a **grid of focusing mirrors** to collect the light. Occasionally, a cascade will occur in a place where two fluorescence detectors can record it, which allows for very precise measurements of the direction the cosmic ray came from.

Fluorescence Detector

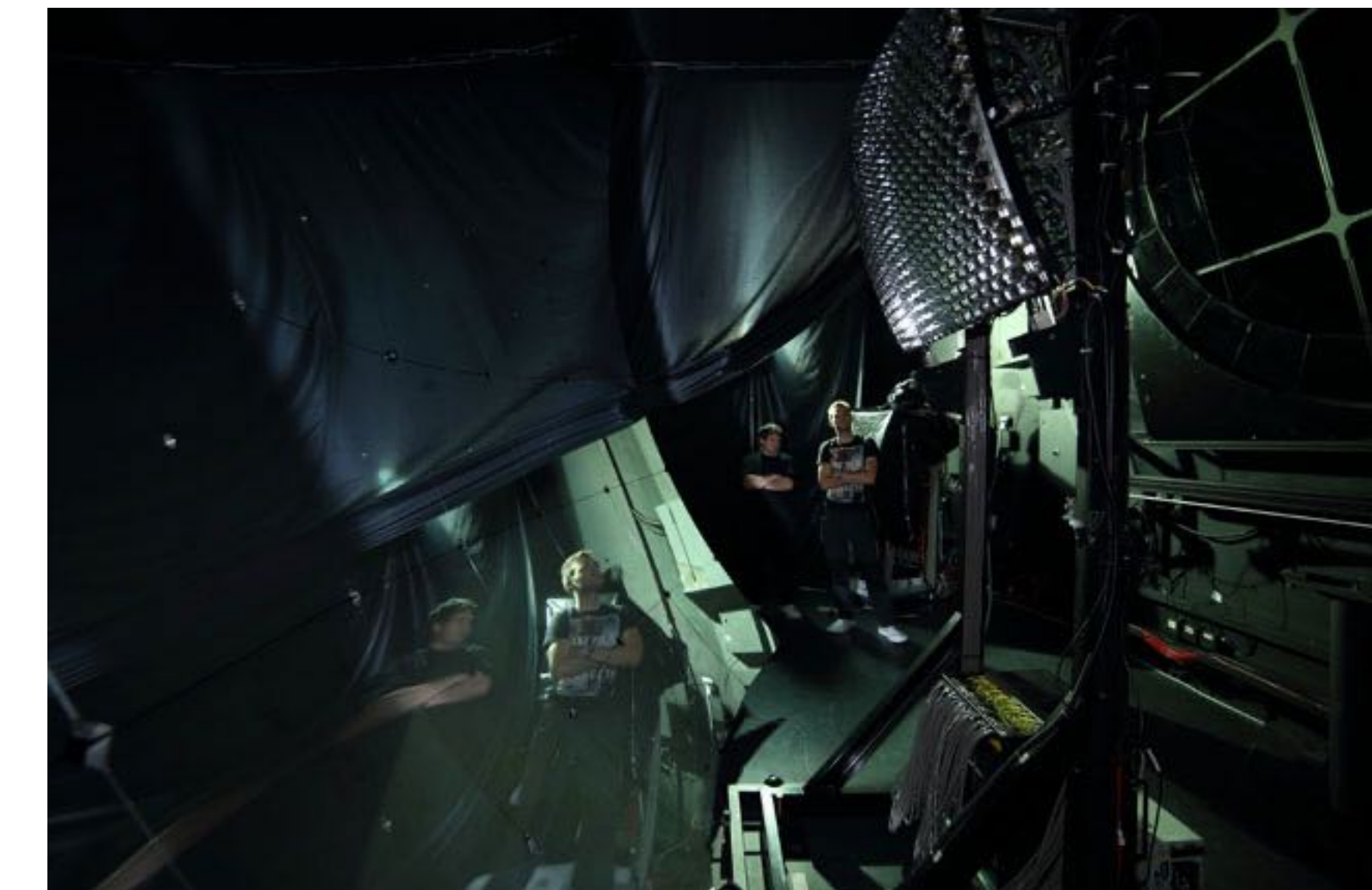
27 fluorescence telescopes
(in 4 different places)



- Mirror surface: 3.6 m x 3.6 m (spherical)
- Opening: 30° x 30°
- Camera: 80 cm x 80 cm



- 440 Photomultipliers
- Detection of fluorescence light
- Range: > 30 km (for 10²⁰ eV air shower)



Interactions used for particle detection

For high energies, the **bremsstrahlung** process becomes significant. The energy loss of electrons due to this process can be described by

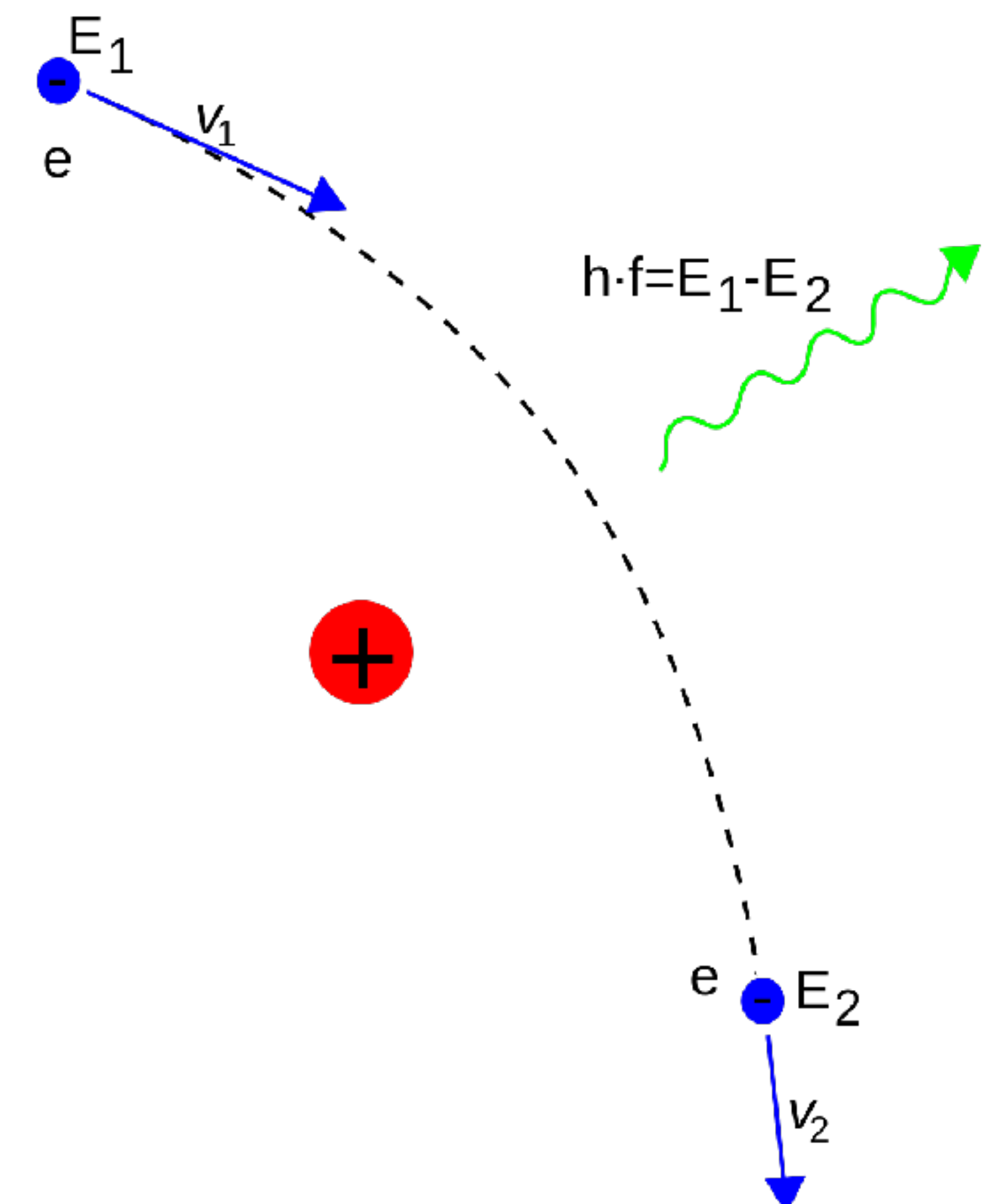
$$-\frac{dE}{dx} \Big|_{\text{brems}} = 4\alpha N_A \frac{Z^2}{A} r_e^2 E \ln \frac{183}{Z^{1/3}} = \frac{E}{X_0}$$

where α is the fine-structure constant ($\alpha^{-1} \approx 137$). The *radiation length is X_0* .

Energy loss due to bremsstrahlung is of particular importance for electrons. For heavy particles, the bremsstrahlung energy loss is suppressed by the factor $1/m^2$. The energy loss, however, increases linearly with energy, and is therefore **important for all particles at high energies**.

Bremsstrahlung

- A Bremsstrahlung, from bremsen "to brake" and Strahlung "radiation"; i.e., "braking radiation" or "**deceleration radiation**", is electromagnetic radiation produced by the deceleration of a charged particle when deflected by another charged particle, typically an electron by an atomic nucleus.
- The moving particle loses kinetic energy, which is converted into radiation (i.e., photons), thus satisfying the law of conservation of energy.
- Bremsstrahlung has a continuous spectrum, which becomes more intense and whose peak intensity shifts toward higher frequencies as the change of the energy of the decelerated particles increases.



Interactions used for particle detection

In addition to bremsstrahlung, charged particles can also lose some of their energy by **direct electron–positron pair production, or by nuclear interactions**. The energy loss due to these two interaction processes also varies linearly with energy.

Muons as secondary particles in astroparticle physics play a **dominant role in particle-detection techniques**, e.g., in neutrino astronomy. **Muons** are not subject to strong interactions and they can consequently travel relatively large distances. This makes them important for particle detection in astroparticle physics. The total **energy loss of muons** can be described by:

$$-\frac{dE}{dx} \Big|_{\text{muon}} = a(E) + b(E) E ,$$

where $a(E)$ describes the **ionization energy loss**, and $b(E) E$ summarizes the processes of **muon bremsstrahlung, direct electron pair creation, and nuclear interaction**. The energy loss of muons in standard rock depends on their energy. It is displayed in Fig. 4.6.

Interactions used for particle detection

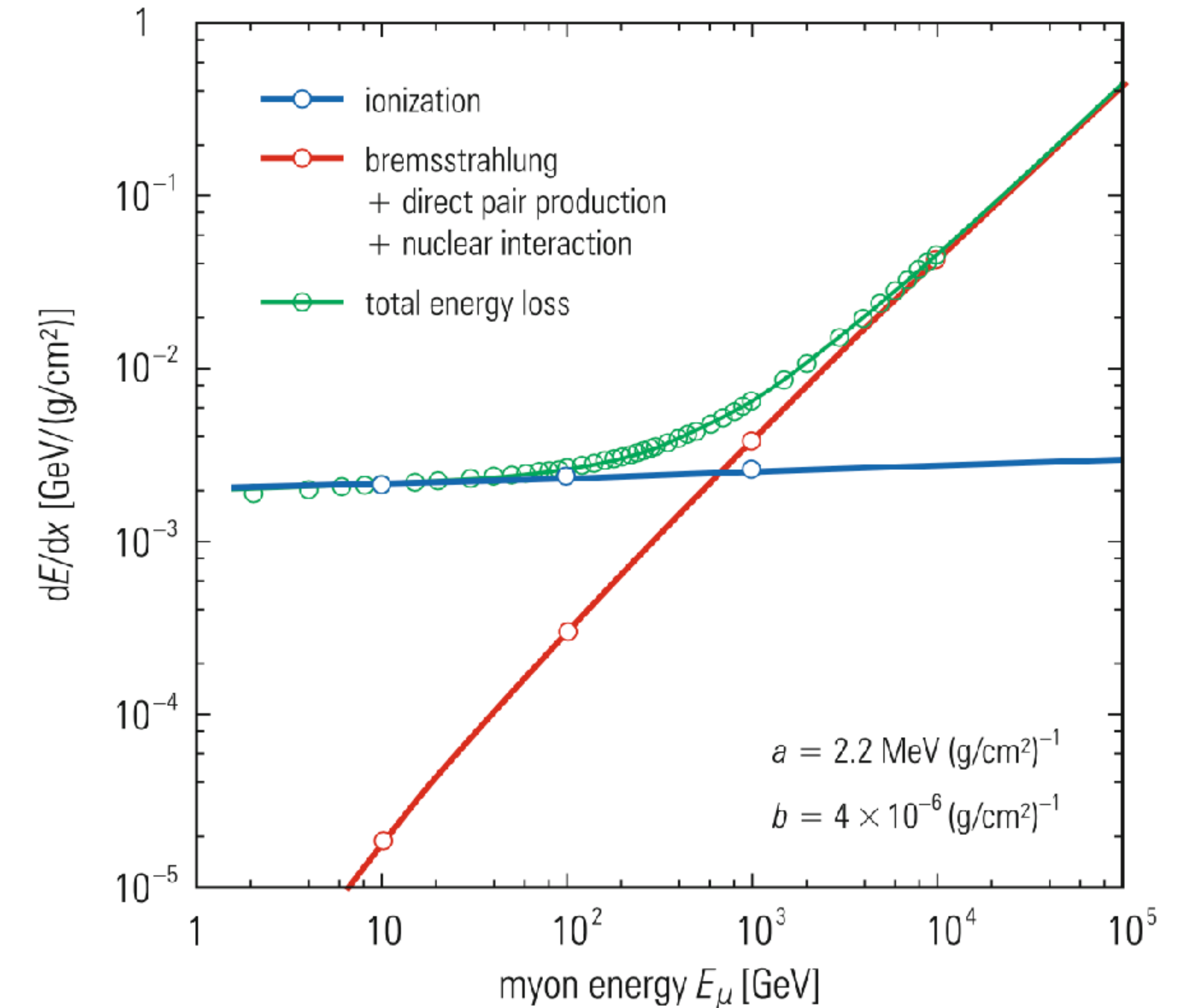


Fig. 4.6 Energy loss of muons in standard rock [34]

Interactions used for particle detection

For particles with high energies, the total energy loss is dominated by bremsstrahlung and the **processes that depend linearly on the particles' energies**. These energy-loss mechanisms are therefore used as a **basis for particle calorimetry**.

In calorimetric techniques, the **total energy of a particle is dissipated in an active detector medium**. The **output signal of such a calorimeter is proportional to the absorbed energy**.

In this context, electrons and photons with energies exceeding **100MeV can already be considered as high-energy particles because they initiate electromagnetic cascades**.

The mass of the muon is much larger than that of the electron, making ***muon calorimetry*** via energy-loss measurements **only possible for energies beyond ≈ 1 TeV**. This calorimetric technique is of particular importance in the field of TeV neutrino astronomy.

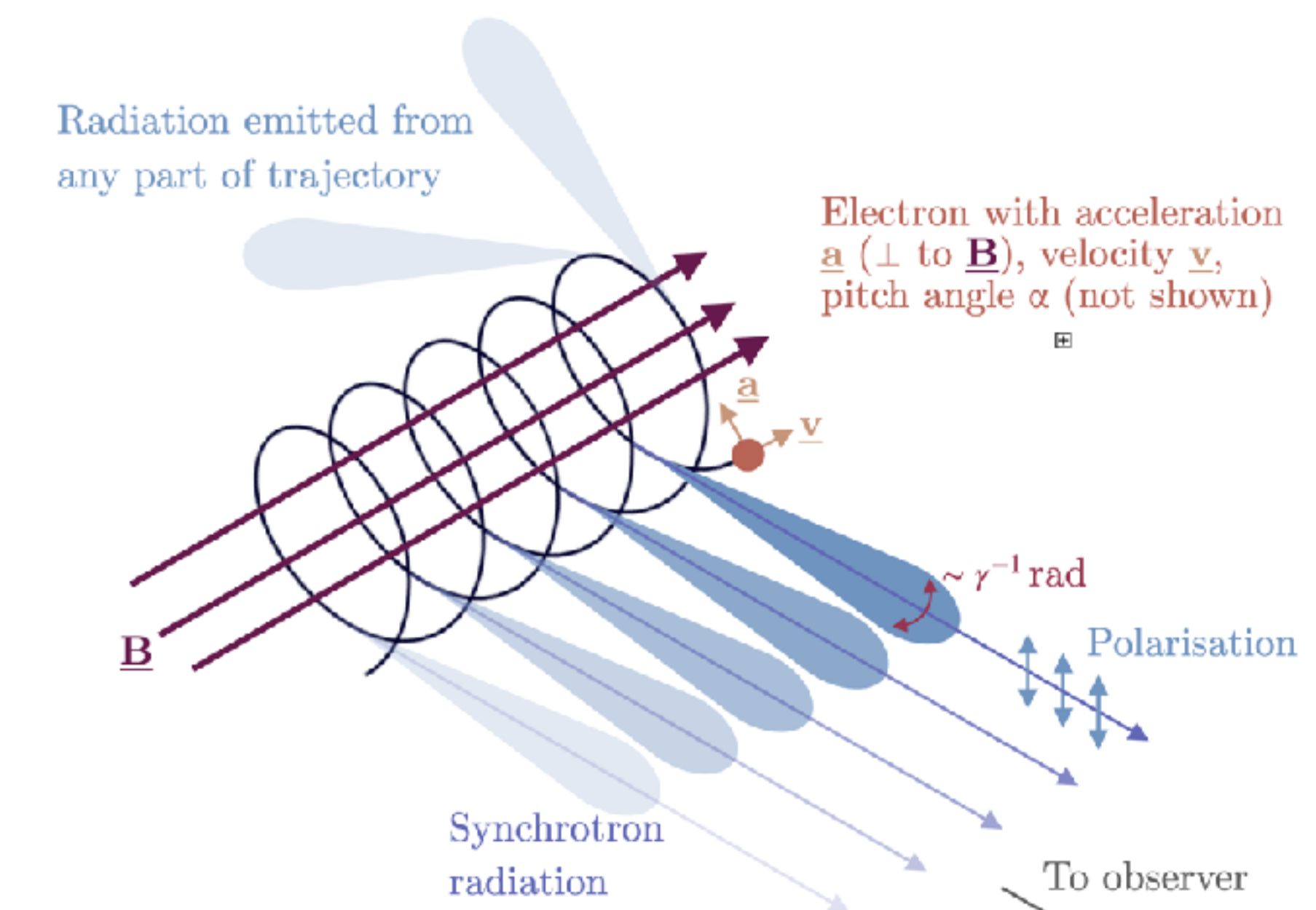
Interactions used for particle detection

Another interaction mechanism, which can be sometimes rather annoying at accelerators and storage rings has recently been used to an advantage in experiments on extensive air showers. The **large number of charged particles created in air showers are deflected in the Earth's magnetic field** and **produce synchrotron radiation**, which is emitted in the **radio domain**.

This **geosynchrotron radiation** allows to investigate air showers with a duty time of 100%, in contrast to the measurements of air showers using the fluorescence technique, which can only be done in the dark and even requires moonless nights.

Synchrotron radiation

- **Synchrotron radiation is the electromagnetic radiation emitted when relativistic charged particles are subject to an acceleration perpendicular to their velocity.** It is produced naturally by fast electrons moving through magnetic fields. The radiation produced in this way has a characteristic polarization and the frequencies generated can range over a large portion of the electromagnetic spectrum.
- Synchrotron radiation is similar to bremsstrahlung radiation, which is emitted by a charged particle when the acceleration is parallel to the direction of motion.
- The **general term for radiation emitted by particles in a magnetic field is gyromagnetic radiation**, for which synchrotron radiation is the ultra-relativistic special case. Radiation emitted by charged particles moving non-relativistically in a magnetic field is called cyclotron emission. For particles in the mildly relativistic range ($\approx 85\%$ of the speed of light), the emission is termed gyro-synchrotron radiation.



Rutha Alexander

Particle identification

Identification means that the **mass of the particle and its charge is determined**. In elementary particle physics most particles have unit charge. But in the study, e.g., of the chemical composition of primary cosmic rays **different charges must be distinguished**.

Every effect of particles or radiation can be used as a working principle for a particle detector.

The **deflection of a charged particle in a magnetic field determines its momentum p** ; the **radius of curvature ρ** is given by

$$\rho \propto \frac{p}{z} = \frac{\gamma m_0 \beta c}{z}$$

where z is the particle's charge, m_0 its rest mass, and $\beta = \frac{v}{c}$ its velocity. The quantity $\frac{p}{z}$ known in astroparticles physics is often called ***magnetic rigidity*** or, simply, *rigidity*.

Particle identification

The particle velocity can be determined, e.g., by a time-of-flight method yielding

$$\beta \propto \frac{1}{\tau}$$

where **τ is the flight time**, which can be measured with a pair of scintillation counters or resistive plate chambers. Also the determination of the Cherenkov angle allows to obtain the particle velocity.

The **Cherenkov angle** is zero at the threshold velocity for the emission of Cherenkov radiation. The angle takes on a maximum as the particle speed approaches the speed of light. Hence, observed angles of incidence can be used to compute the direction and speed of a Cherenkov radiation-producing charge.

Particle identification

In the figure on the geometry, the particle (red arrow) travels in a medium with speed $\frac{c}{n} < v_p < c$

where **n is the refractive index of the medium**. If the medium is water, the condition is $0.75c < v_p < c$, since $n \approx 1.33$ (air: $n \approx 1$) for water at 20°C .

The emitted light waves (denoted by blue arrows) travel at speed

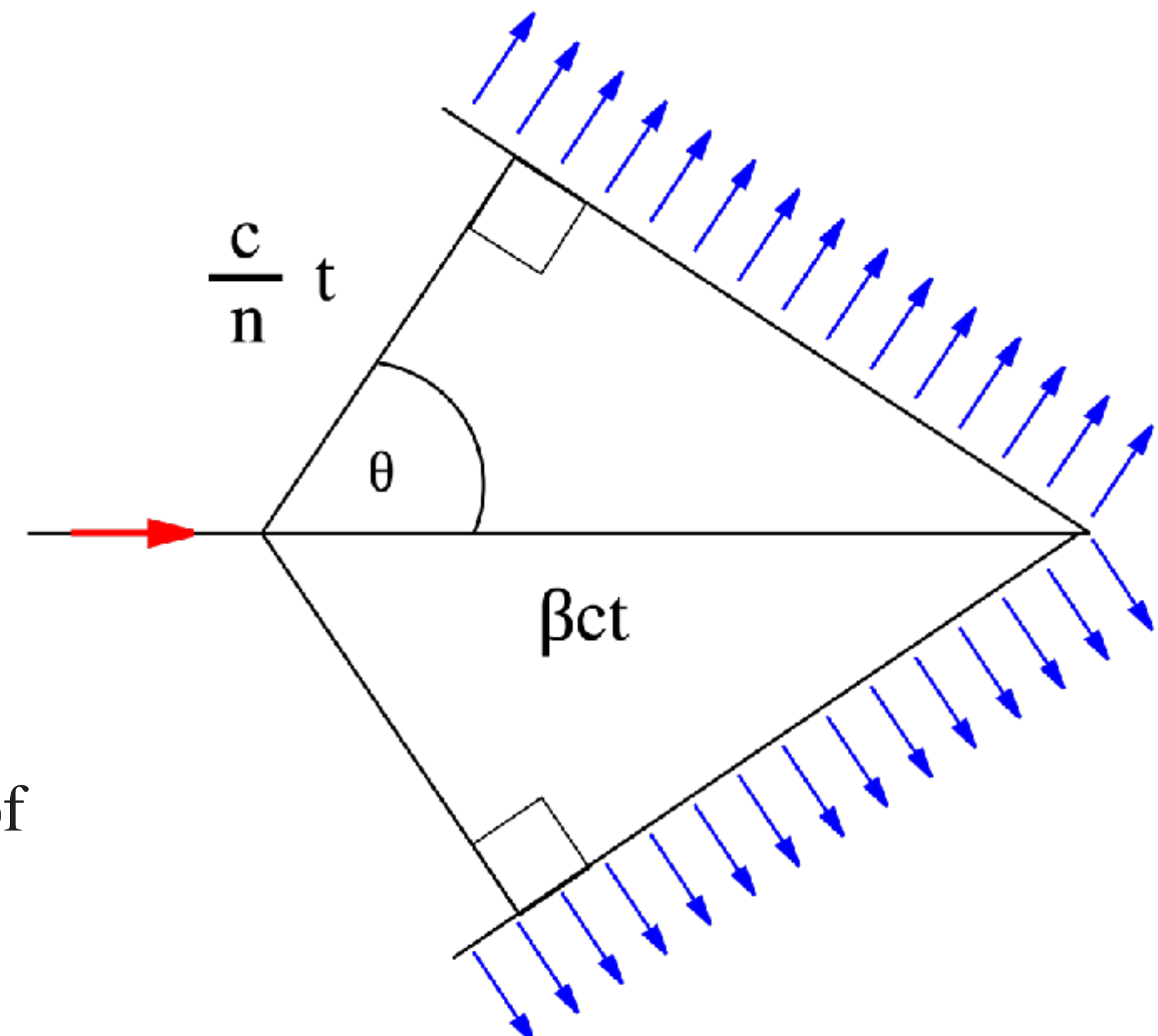
$$v_{em} = \frac{c}{n}$$

The left corner of the triangle represents the location of the superluminal particle at some initial moment ($t = 0$). The right corner of the triangle is the location of the particle at some later time t . In the given time t , the particle travels the distance $x_p = v_p t = \beta c t$

whereas the emitted electromagnetic waves are constricted to travel the

$$\text{distance } x_{em} = v_{em} t = \frac{c}{n} t$$

So the emission angle results in $\theta_C = \frac{1}{n\beta}$



Particle identification

A calorimetric measurement provides a determination of the kinetic energy

$$E^{\text{kin}} = (\gamma - 1)m_0c^2$$

$$\gamma = \frac{1}{\sqrt{1 - \beta^2}}$$
 Lorentz factor.

From these measurements the ratio of m_0/z can be inferred, i.e., for singly charged particles we have already identified the particle. To determine the charge one needs another **z -sensitive effect, e.g., the ionization energy loss**

$$\frac{dE}{dx} \propto \frac{z^2}{\beta^2} \ln(a\beta\gamma)$$

(a is a material-dependent constant).

Particle identification

Now we know m_0 and z separately. In this way even different isotopes of elements can be distinguished.

Neutral particles can only be identified via their interaction products. If all particles produced in such an interaction are measured the identity of the neutral particle can be determined.

A particular case are **neutrinos in a final state of an interaction**. Neutrinos leave no tracks in the detector, but if the **total energy of the final-state particles is known**, e.g., as decay products of a heavy particle, **neutrinos can be reconstructed from the missing energy and missing momentum and thereby also identified**.

Atmospheric air Cherenkov technique

The atmospheric Cherenkov technique is becoming increasingly popular for **TeV γ astronomy** since it allows to identify **photon-induced electromagnetic showers**, which develop in the atmosphere. A charged particle that moves in a medium with refractive index n , and has a velocity v that exceeds the velocity of light $c_n = c/n$, emits electromagnetic radiation known as **Cherenkov radiation**.

There is a **threshold effect** for this kind of energy loss; Cherenkov radiation only occurs if

$$v \geq \frac{c}{n} \text{ or, equivalently, } \beta = \frac{v}{c} \geq \frac{1}{n}$$

Cherenkov radiation is emitted under an angle of

$$\theta_C = \arccos \frac{1}{n\beta}$$

relative to the direction of the particle velocity.

Atmospheric air Cherenkov technique

Due to this process, a particle of charge number z creates a certain number of photons in the visible spectral range ($\lambda_1 = 400$ nm up to $\lambda_2 = 700$ nm). The **number of photons produced per centimeter** is calculated from the following equation:

$$\frac{dN}{dx} = 2\pi\alpha z^2 \frac{\lambda_2 - \lambda_1}{\lambda_1 \lambda_2} \sin^2 \theta_C$$
$$\approx 490 z^2 \sin^2 \theta_C \text{ cm}^{-1}.$$

These photons are emitted isotropically in azimuth

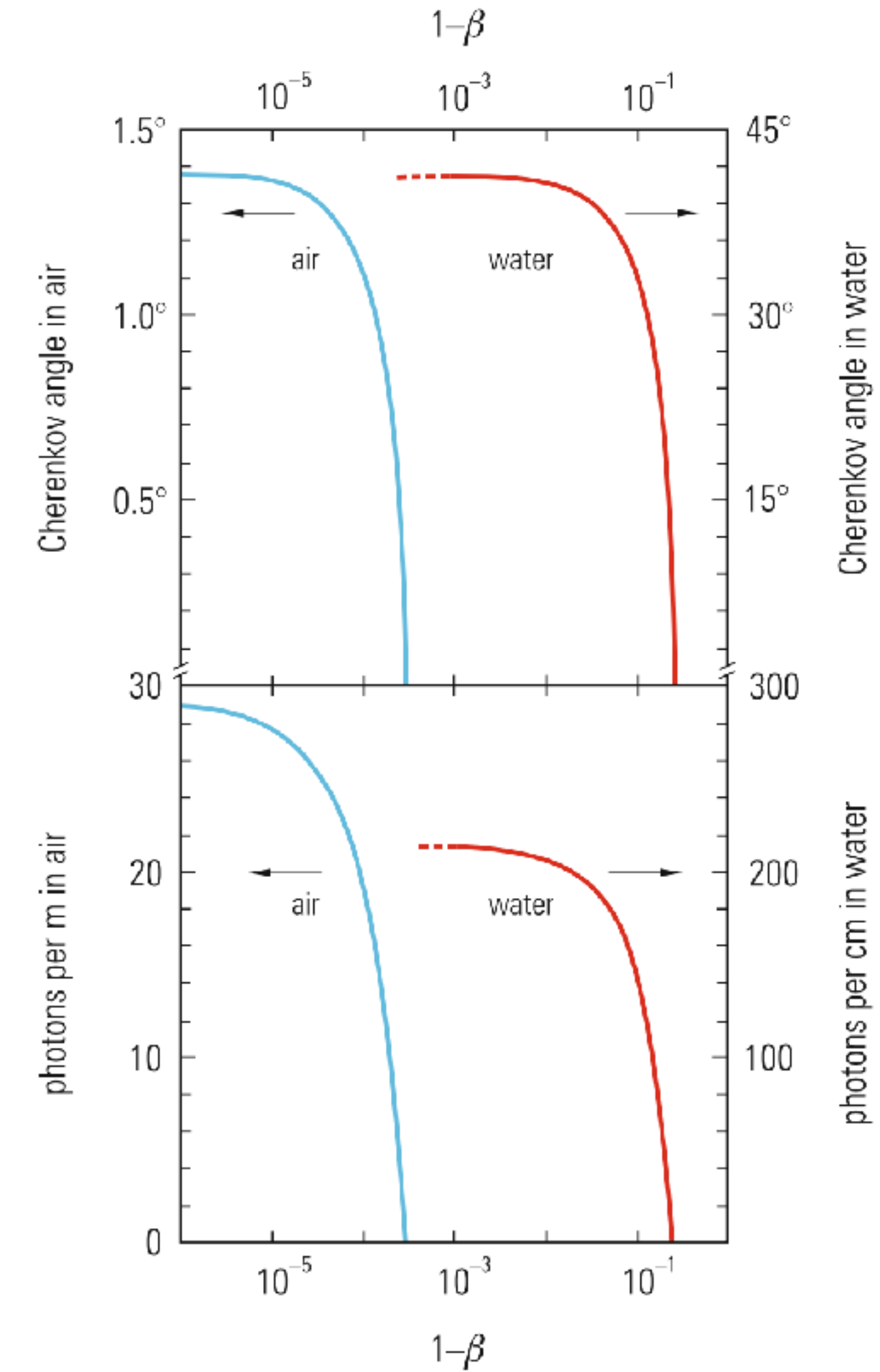


Fig. 4.7 Variation of the Cherenkov angle and photon yield of singly charged particles in water and air

Atmospheric air Cherenkov technique

For relativistic particles ($\beta \approx 1$), the Cherenkov angle is 42° in water and 1.4° in air (Fig. 4.7).

In water, around 220 photons per centimeter are produced by a singly charged relativistic particle. The corresponding number in air is 30 photons per meter.

Figure 4.7 shows the variation of the Cherenkov angle and the photon yield with the particle velocity for water and air.

The **atmospheric Cherenkov technique permits the identification of photon-induced electromagnetic showers that develop in the atmosphere and separates them from the more abundant hadronic cascades.**

Photons point back to their sources, while hadrons mainly produce only an isotropic background. The axis of the Cherenkov cone follows the direction of incidence of the primary photon. The Cherenkov cone for γ -induced cascades in air spans only $\pm 1.4^\circ$, therefore the hadronic background in such a small angular range is relatively small. Apart from this background subtraction, also the different Cherenkov patterns in the photomultiplier matrix in the recording system, which is characteristically different for hadron and photon or electron induced showers, can be used for particle separation.

Atmospheric air Cherenkov technique

Apart from the atmospheric Cherenkov technique, the Cherenkov effect is also utilized in **large water Cherenkov detectors for neutrino astronomy**.

The operation principle of a water Cherenkov counter is sketched in Fig. 4.8. Cherenkov radiation is emitted along a distance Δx . The Cherenkov cone projects an image on the detector surface, which is at a distance d from the source. The image is a ring with an average radius

$$r = d \tan \theta_C$$

This detection technique plays an important role in the huge experiments like Super-Kamiokande and in ICECUBE.

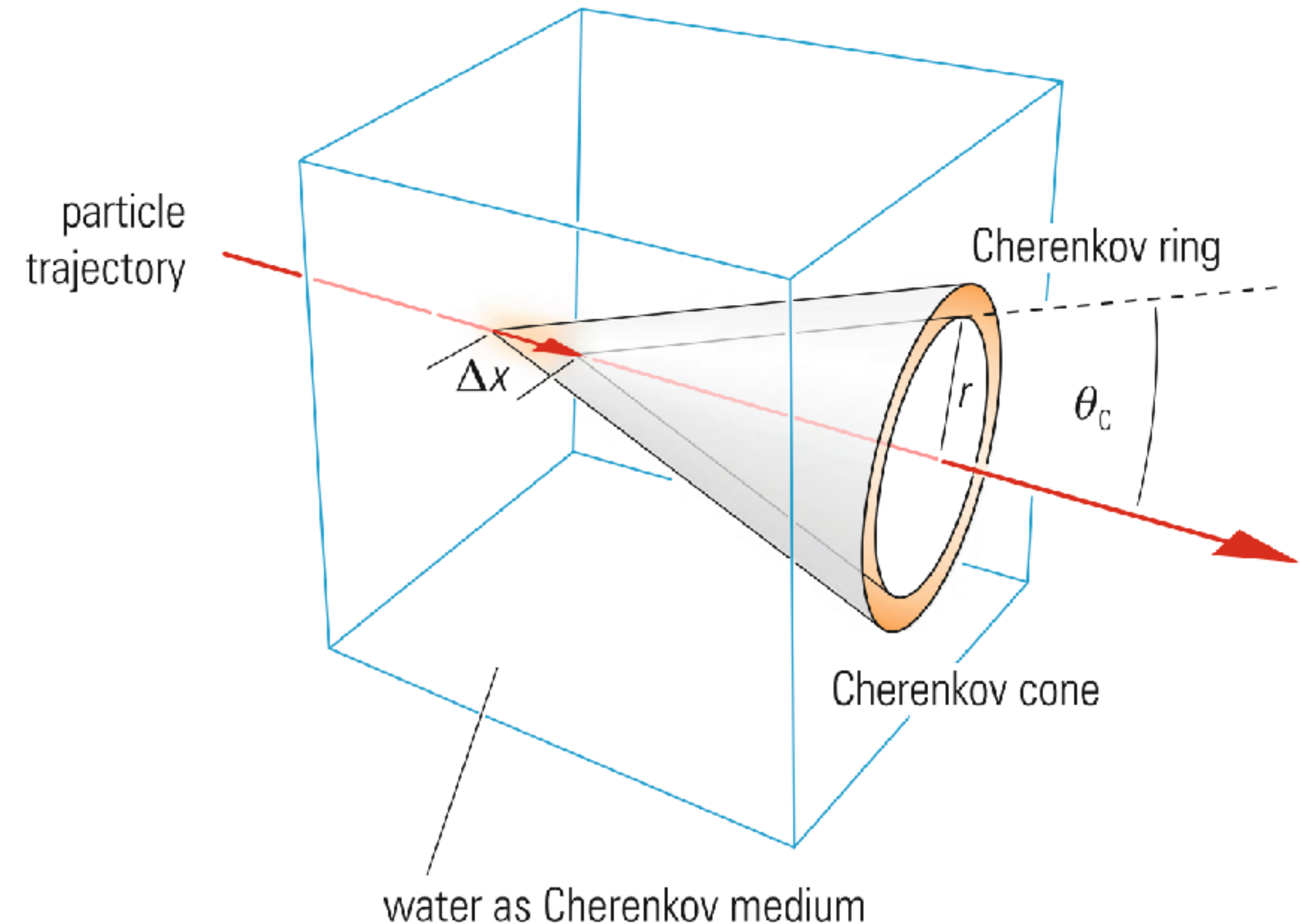


Fig. 4.8 Production of a Cherenkov ring in a water Cherenkov counter

Atmospheric air Cherenkov technique

For **very high energies charged particles** can also be detected via **transition radiation**. They can even be identified with this technique because the intensity or energy, respectively, of the transition-radiation photons depends on the Lorentz factor of the incident particle. This allows, e.g., an electron–pion separation in transition radiation detectors, if the momentum of the particles is known.

Transition radiation (TR) is a form of **electromagnetic radiation emitted when a charged particle passes through inhomogeneous media, such as a boundary between two different media**. This is in contrast to Cherenkov radiation, which occurs when a charged particle passes through a homogeneous dielectric medium at a speed greater than the phase velocity of electromagnetic waves in that medium.

Energy losses of an ultrarelativistic particle, when emitting TR while passing the boundary between media and vacuum, are directly proportional to the Lorentz factor of the particle. This x-ray transition radiation, makes it possible to use TR in high-energy physics.

The emitted radiation is the homogeneous difference between the two inhomogeneous solutions of Maxwell's equations of the electric and magnetic fields of the moving particle in each medium separately.

Atmospheric air Cherenkov technique

In other words, since the electric field of the particle is different in each medium, **the particle has to "shake off" the difference when it crosses the boundary.**

The **total energy loss of a charged particle on the transition depends on its Lorentz factor** and is mostly directed forward, peaking at an angle of the order of $1/\gamma$ relative to the particle's path. **The intensity of the emitted radiation is roughly proportional to the particle's energy E.**

Optical transition radiation is emitted both in the forward direction and reflected by the interface surface. In case of a foil having an angle at 45 degrees with respect to a particle beam, the particle beam's shape can be visually seen at an angle of 90 degrees. More elaborate **analysis of the emitted visual radiation may allow for the determination of γ and emittance.**

In the approximation of relativistic motion ($\gamma \gg 1$), small angles ($\theta \ll 1$) and high frequency ($\omega \gg \omega_p$), the energy spectrum can be expressed as:

$$\frac{dI}{d\nu} \approx \frac{z^2 e^2 \gamma \omega_p}{\pi c} \left((1 + 2\nu^2) \ln\left(1 + \frac{1}{\nu^2}\right) - 2 \right)$$

Atmospheric air Cherenkov technique

Where z is the atomic charge, e is the charge of an electron, γ is the Lorentz factor, ω_p is the Plasma Frequency. This diverges at low frequencies where the approximations fail. The total energy emitted is:

$$I = \frac{z^2 e^2 \gamma \omega_p}{3c}$$

The characteristics of this electromagnetic radiation make it suitable for particle discrimination, particularly of **electrons and hadrons in the momentum range between 1 GeV/c and 100 GeV/c**. The transition radiation photons produced by electrons have wavelengths in the x-ray range, with energies typically in the range from 5 to 15 keV.

However, the number of produced photons per interface crossing is very small: for particles with $\gamma = 2 \times 10^3$, about 0.8 X-ray photons are detected. Usually several layers of alternating materials or composites are used to collect enough transition radiation photons for an adequate measurement—for example, one layer of inert material followed by one layer of detector, and so on.

Special aspects of photon detection

The detection of photons is more indirect compared to charged particles. **Photons first have to create charged particles in an interaction process. These charged particles will then be detected via the processes described, such as ionization, excitation, bremsstrahlung, and the production of Cherenkov radiation.**

At comparatively low energies, as in X-ray astronomy, photons can be imaged by reflections at grazing incidence. Photons are detected in the focal plane of an X-ray telescope via the photoelectric effect. Semiconductor counters, X-ray CCDs, or multiwire proportional chambers filled with a noble gas of high atomic number (e.g., krypton, xenon) can be used for focal detectors. These types of detectors provide spatial details, as well as energy information (see Fig. 4.9).

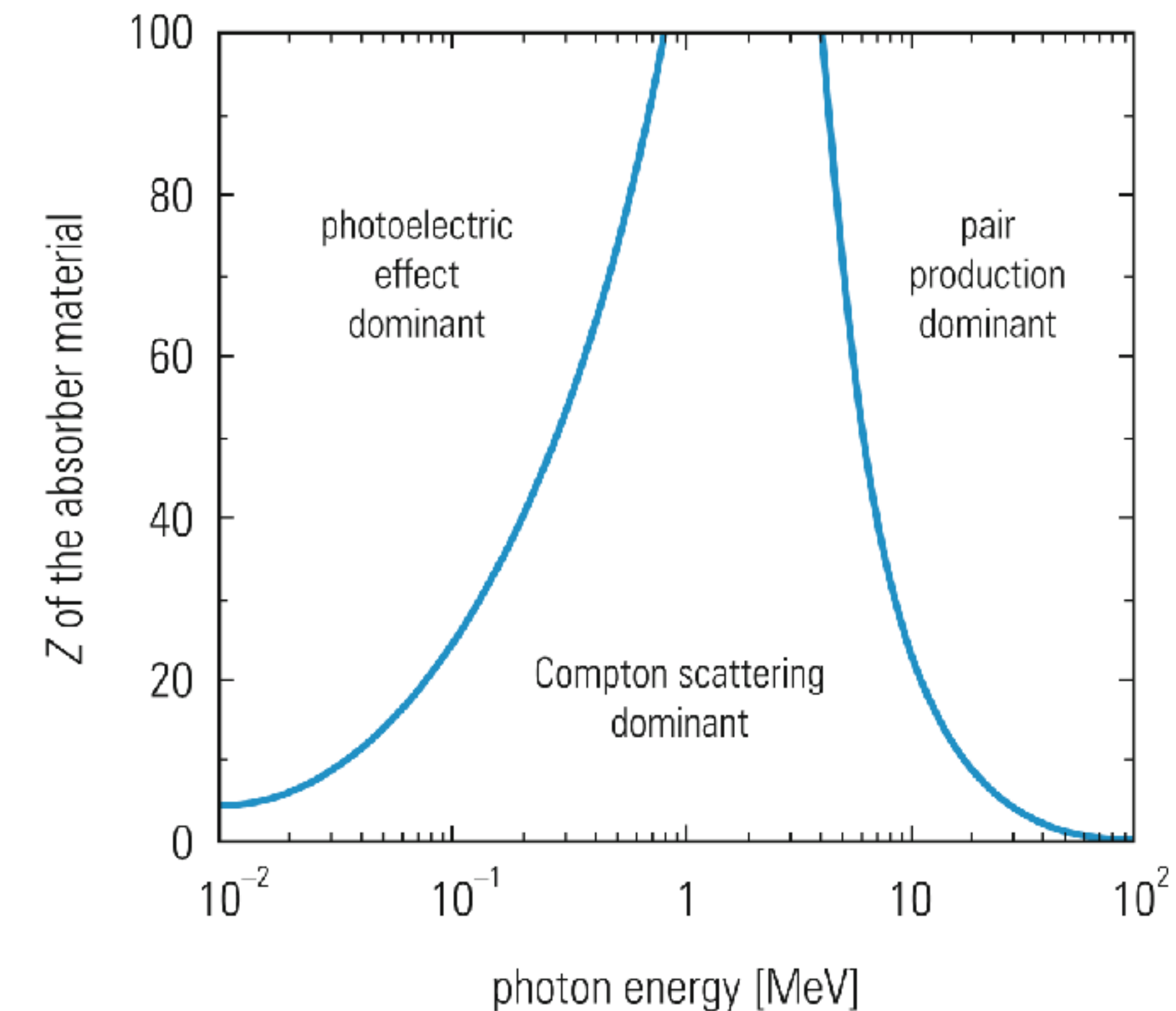
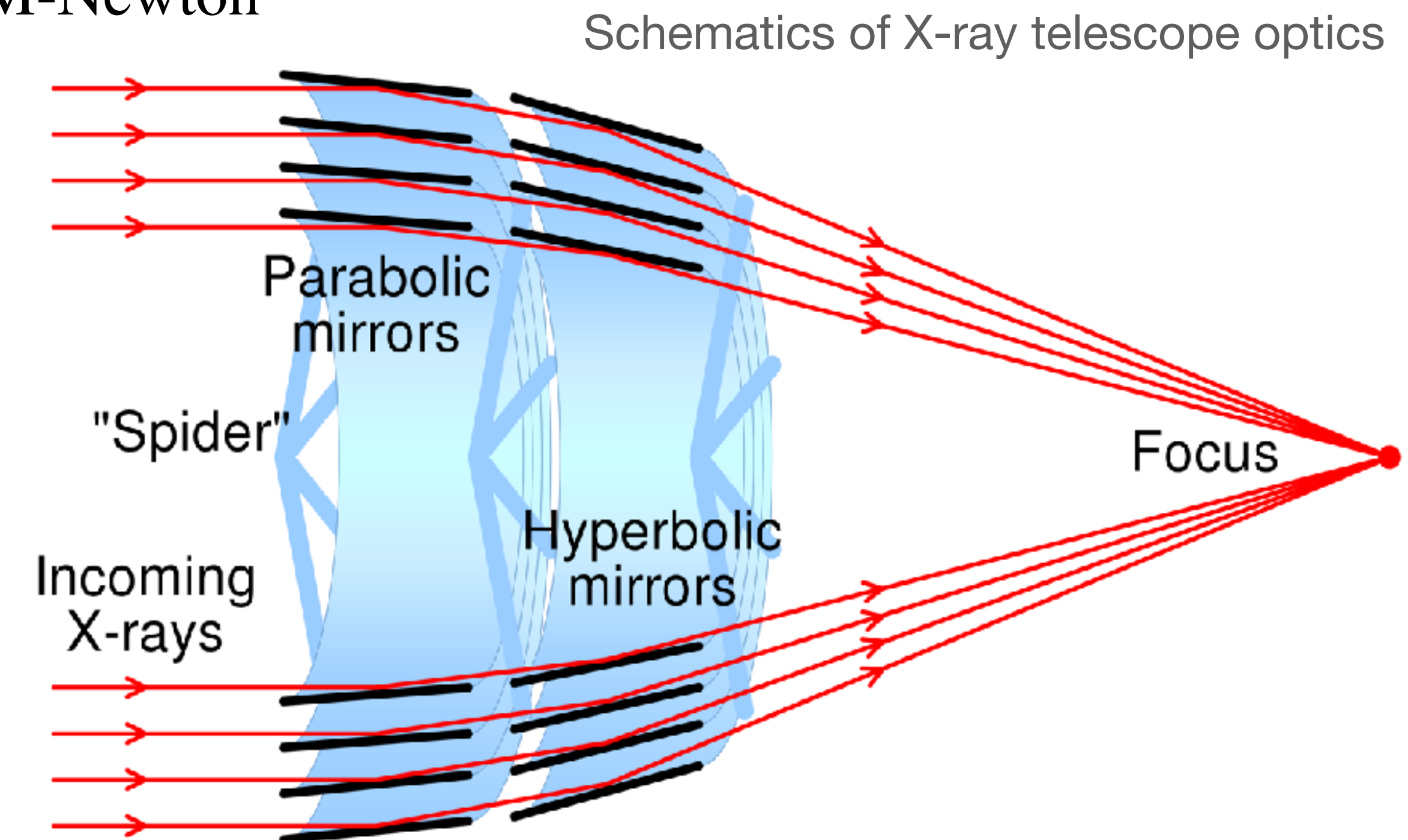


Fig. 4.9 Domains, in which various photon interactions dominate, shown in their dependence on the photon energy and the nuclear charge of the absorber

X - ray astronomy

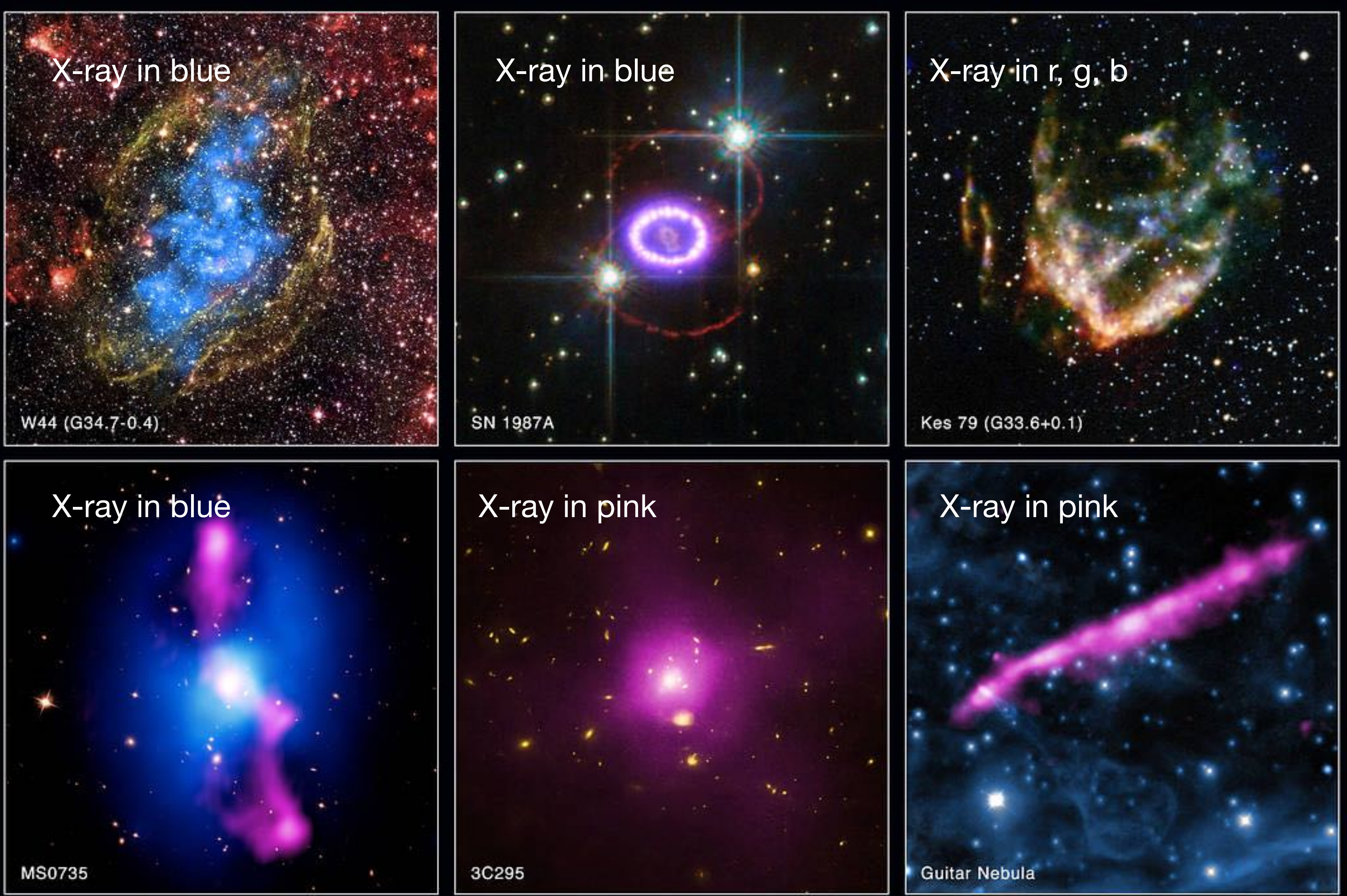
- Only detectable above the atmosphere: balloon experiments and satellites
- X-rays are reflected from metal surfaces only when they are incident at grazing angles (otherwise, they pass through metals). Hence X-ray telescopes are designed very differently from optical telescopes.
- Mirrors in X-ray telescopes have to be much smoother than mirrors in optical telescopes because of the small wavelength of X-rays.
- Examples for X-ray telescopes: ROSAT, Chandra, XMM-Newton



X - ray astronomy

Composit images with Chandra X-ray data

- Sources: hot plasma (millions of K)
- Examples: the Sun, Supernova remnants, intra cluster matter in galaxy clusters, AGN, accreting binary stars, neutron star or black hole binaries.

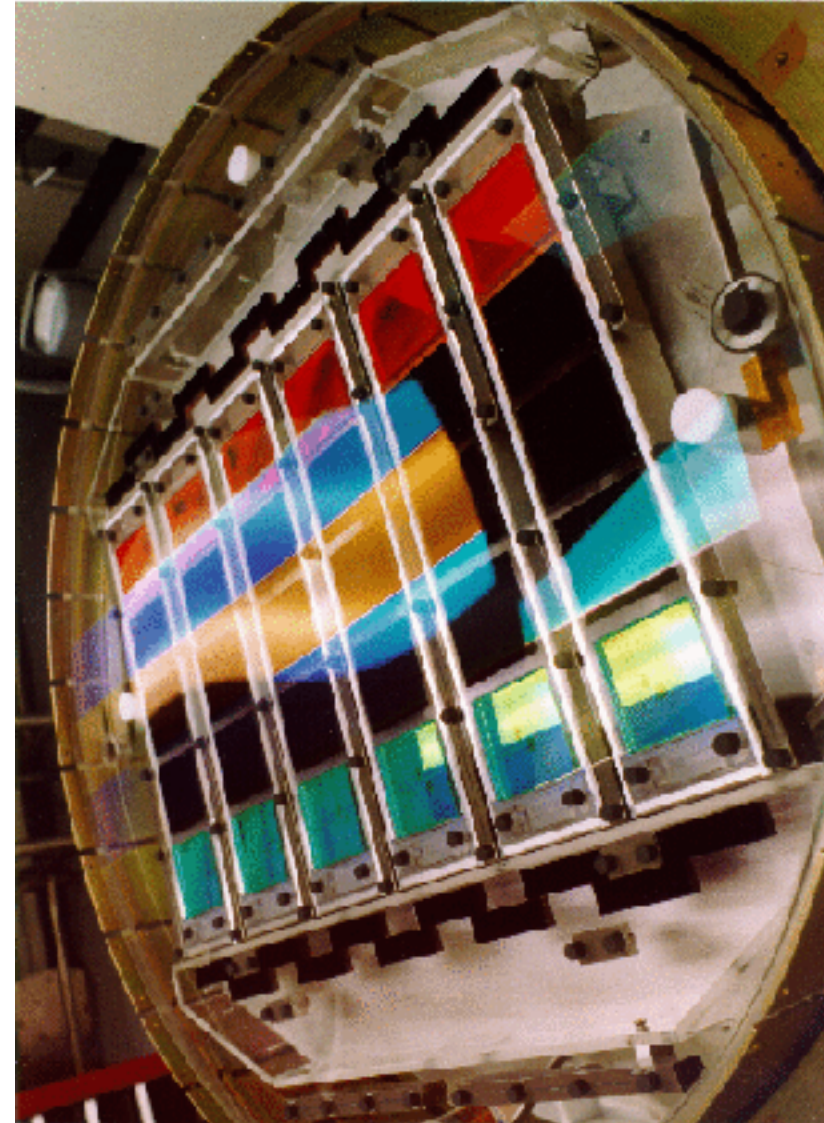


CCD detectors

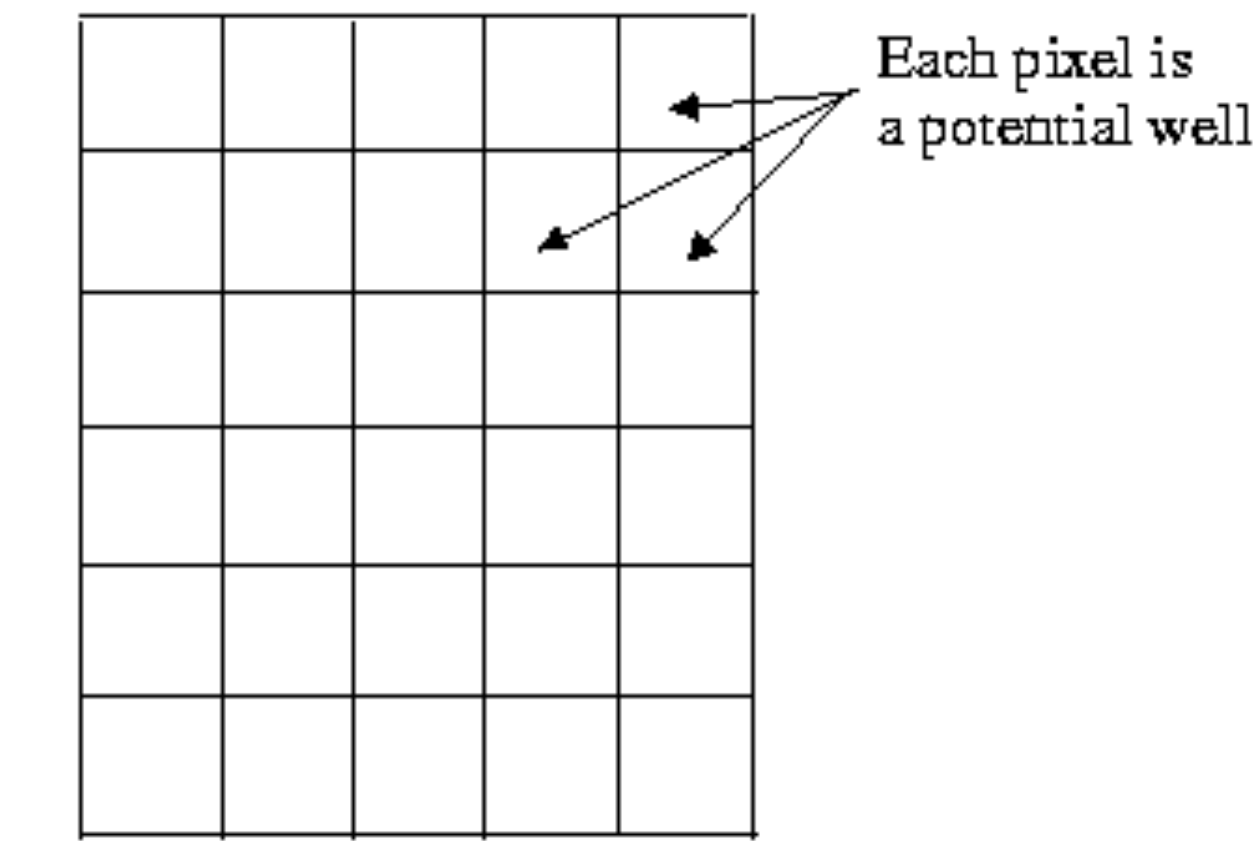
- A Charge Coupled Device (**CCD**) is a highly sensitive **photon detector**. The CCD is divided up into a large number of light-sensitive small areas (known as pixels) which can be used to build up an image.
- **A photon of light which falls within the area defined by one of the pixels will be converted into one (or more) electrons and the number of electrons collected will be directly proportional to the intensity of the light at each pixel.**
- When the CCD is clocked out, the number of electrons in each pixel are measured and the image can be reconstructed.
- A CCD will consist of a large number of pixels, arranged horizontally in rows and vertically in columns.
- A CCD treats light as “particles” - only the intensity of the radiation is measured.
- Used for nearly all UV, optical and infrared telescopes, also used for X-rays.



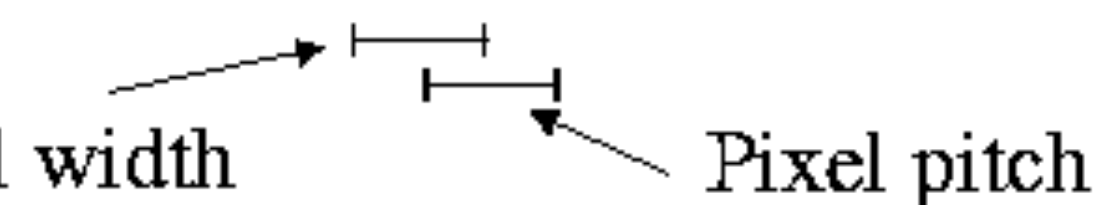
An array of 30 CDD chips from the Sloan Digital Sky Survey



Horizontal rows

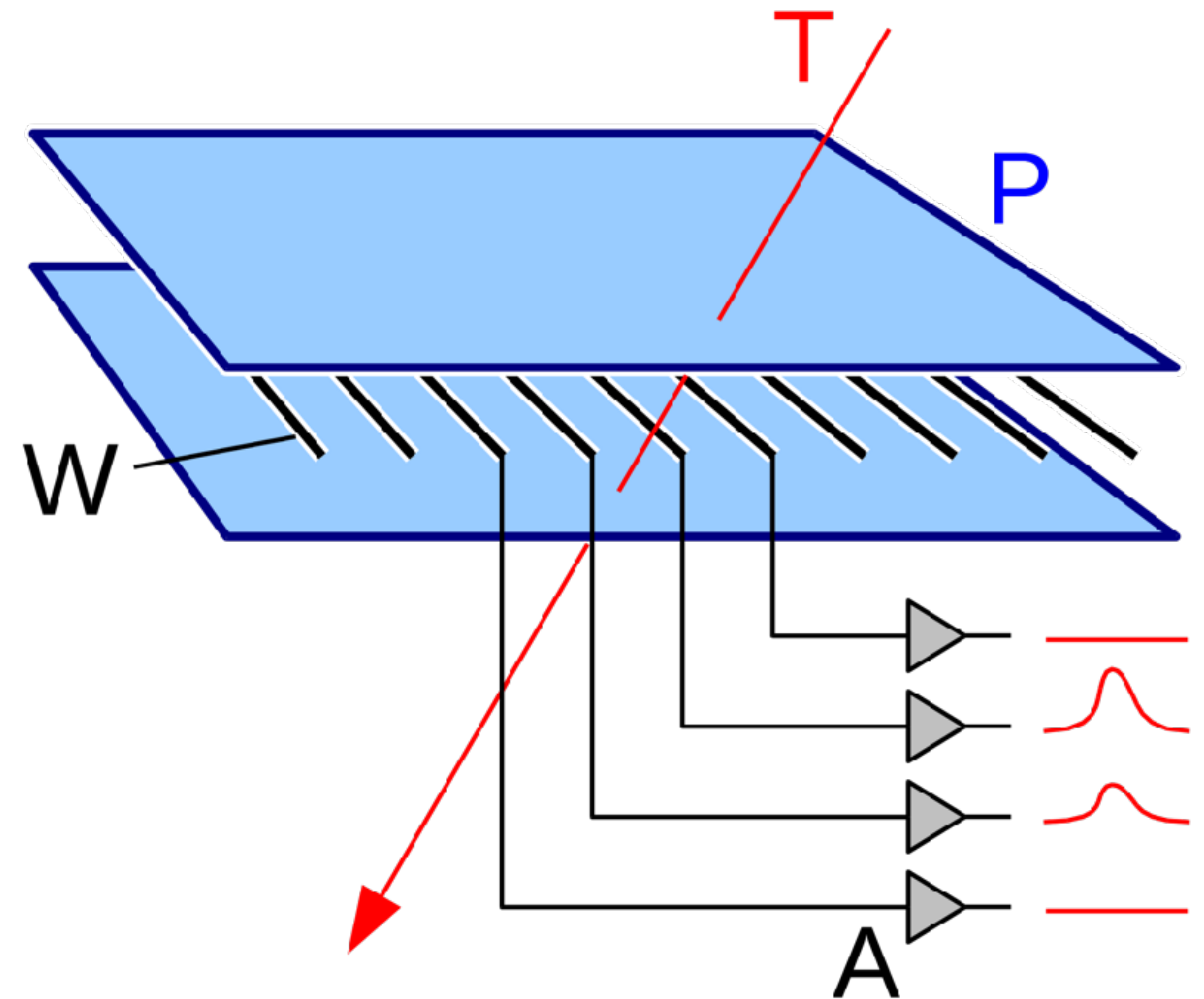


Vertical columns



Multi wire chamber

A wire chamber or **multi-wire proportional chamber** is a type of proportional counter that detects charged particles and photons and can give positional information on their trajectory, by tracking the trails of gaseous ionization.



Wire chamber with wires (W) and cathode (–) plates (P). The particles traveling along trajectory T will ionize gas atoms and set free a charge that an amplifier (A) collects (impulse at the output).

Special aspects of photon detection

The **Compton effect dominates for photons at MeV energies** (see Fig. 4.9). In *Compton scattering*, a photon of energy E_γ transfers part of its energy ΔE to a **target electron, thereby being redshifted**. Based on the reaction kinematics, the ratio of the scattered photon energy E'_γ to the incident photon energy E_γ can be derived:

$$\frac{E'_\gamma}{E_\gamma} = \frac{1}{1 + \varepsilon(1 - \cos \theta_\gamma)}$$

In this equation, $\varepsilon = E_\gamma/m_e c^2$ is the reduced photon energy and θ_γ is the scattering angle of the photon in the γ – electron interaction (Fig. 4.10).

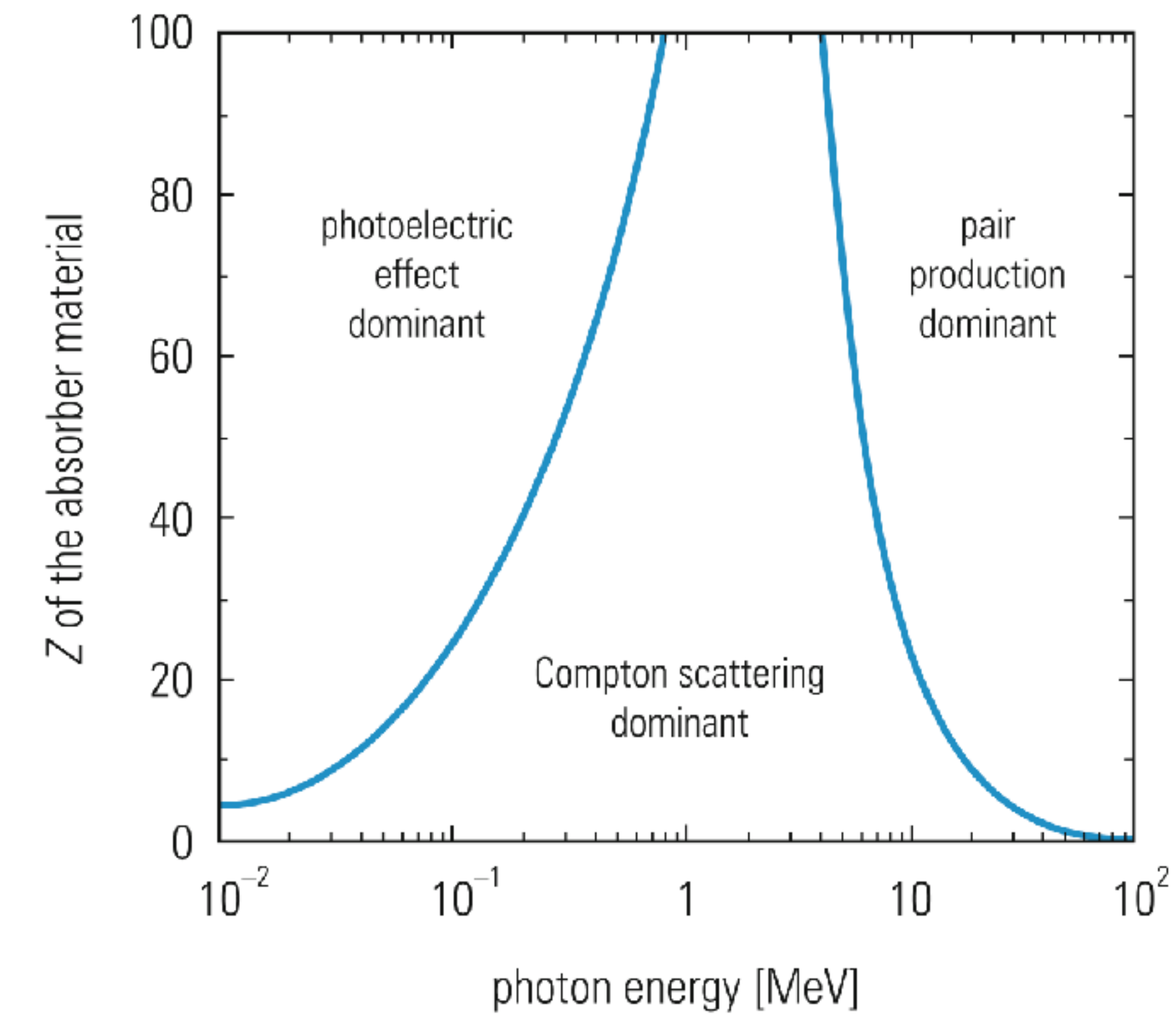


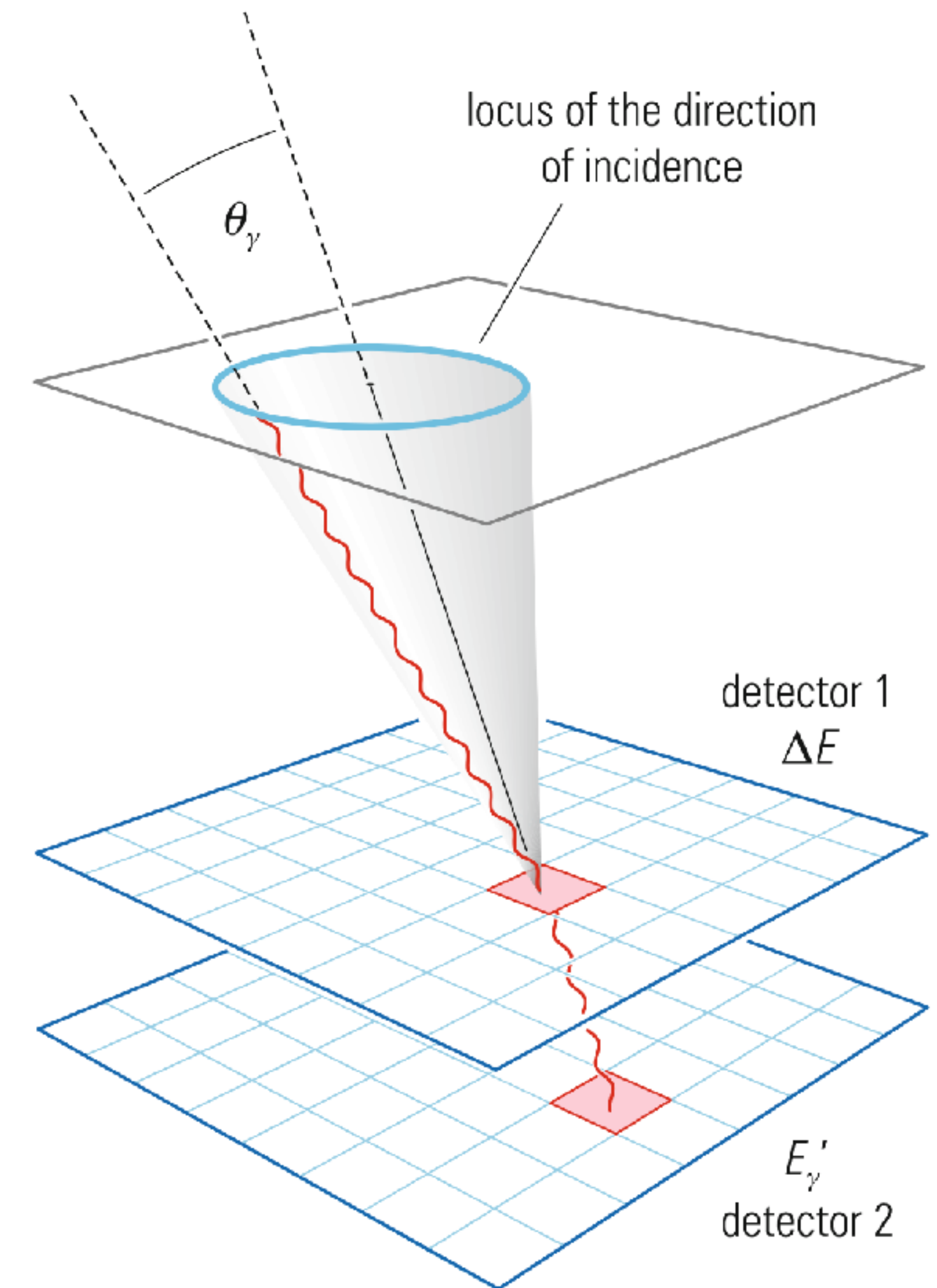
Fig. 4.9 Domains, in which various photon interactions dominate, shown in their dependence on the photon energy and the nuclear charge of the absorber

Special aspects of photon detection

Fig. 4.10 Principle of a Compton telescope

With a Compton telescope, not only the **energy**, but **also the direction** of incidence of the photons **can be determined**. In such a telescope, the energy loss of the Compton-scattered photon $\Delta E = E_\gamma - E'_\gamma$ is determined in the upper detector layer by measuring the energy of the Compton electron (see Fig. 4.10).

The Compton-scattered photon of reduced energy will subsequently be detected in the lower detector plane, preferentially by the photoelectric effect. Based on the kinematics of the scattering process and using (4.5.1), the scattering angle θ_γ can be determined.

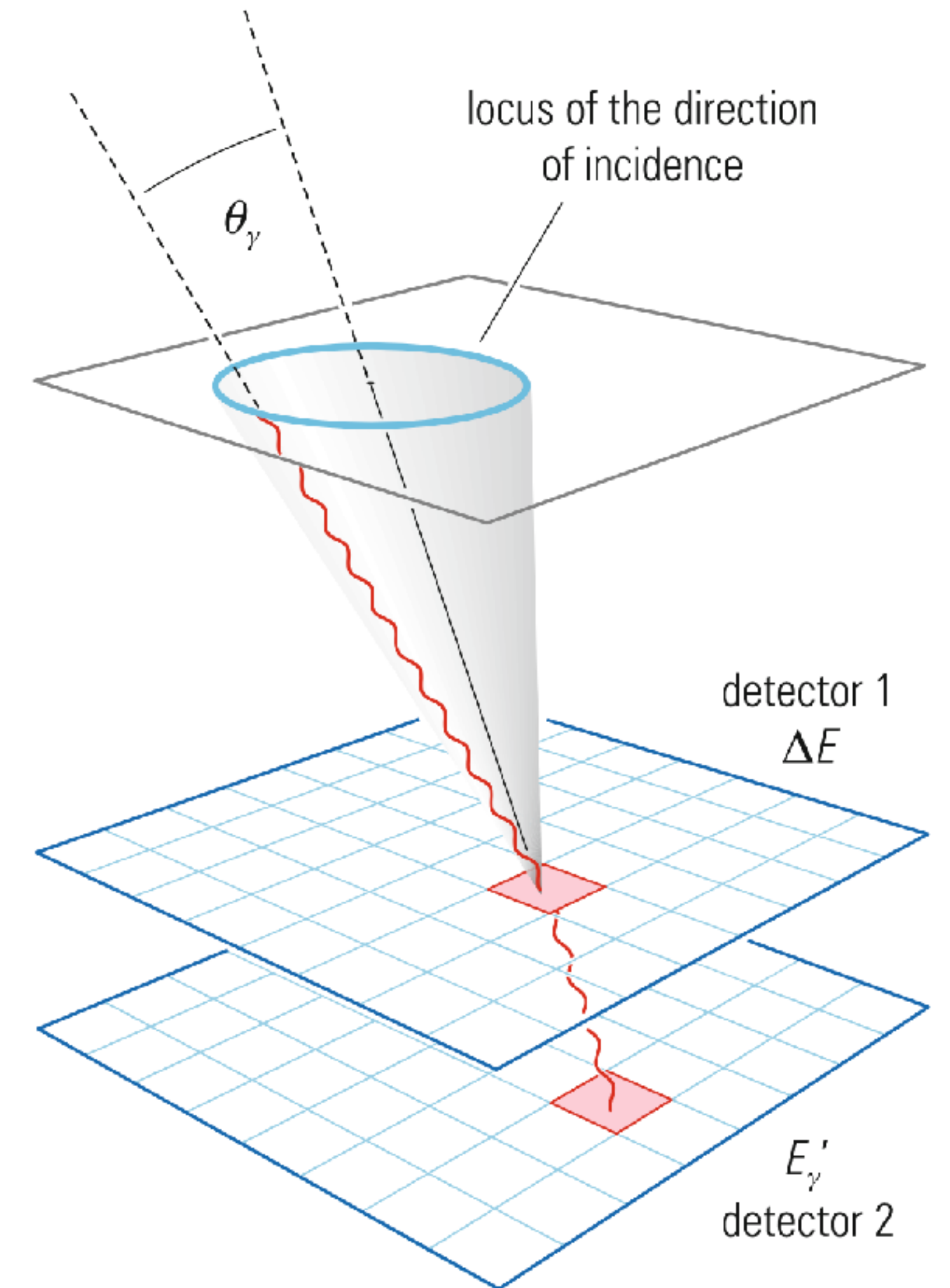


Special aspects of photon detection

Fig. 4.10 Principle of a Compton telescope

As a consequence of the isotropic emission around the azimuth, the reconstructed photon direction does not point back to a unique position in the sky; it only defines a circle, respectively ellipse, in the sky. **If, however, many photons are recorded from the source, the intercepts of these circles (or ellipses) define the position of the source.** The detection of photons via the Compton effect in such Compton telescopes is usually performed using segmented large-area inorganic or organic scintillation counters that are read out via photomultipliers.

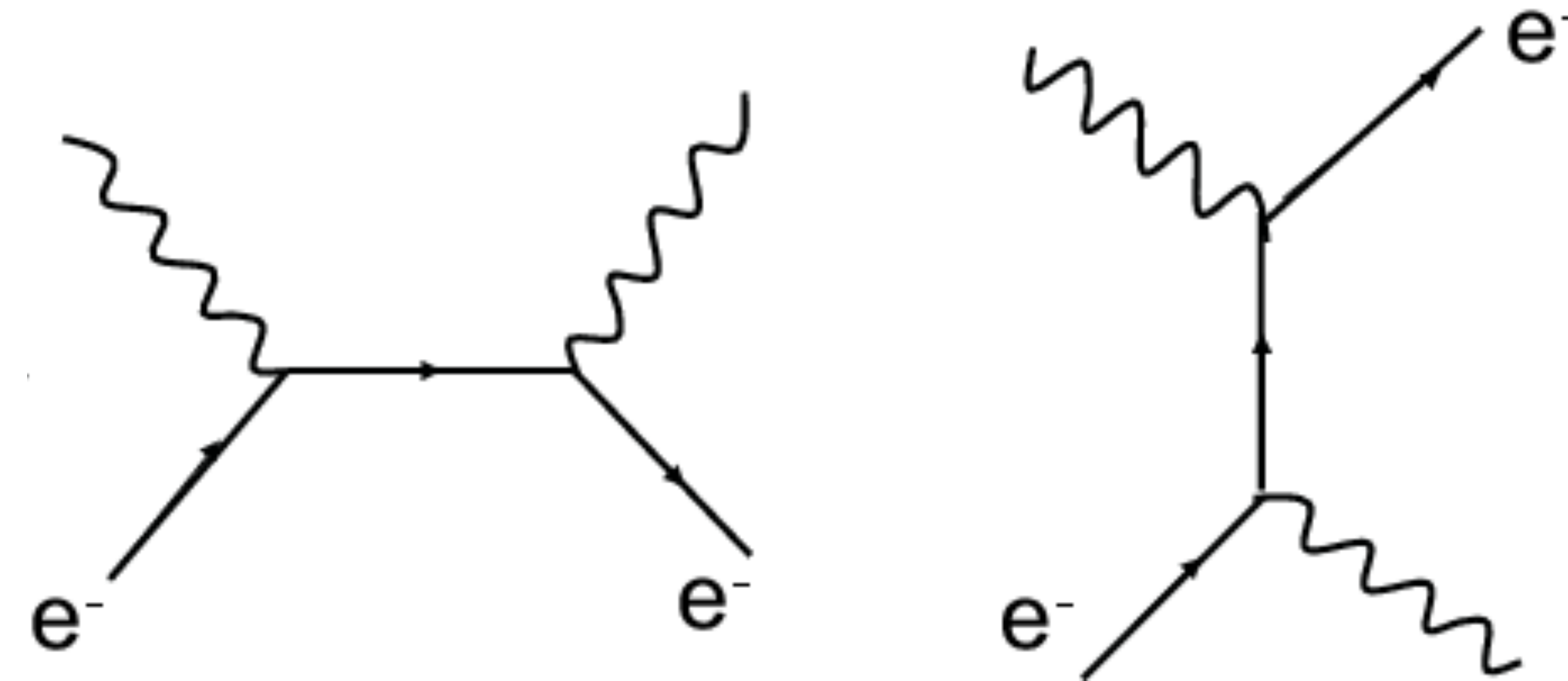
Alternatively, for high-resolution telescopes, semiconductor pixel detectors can also be used.



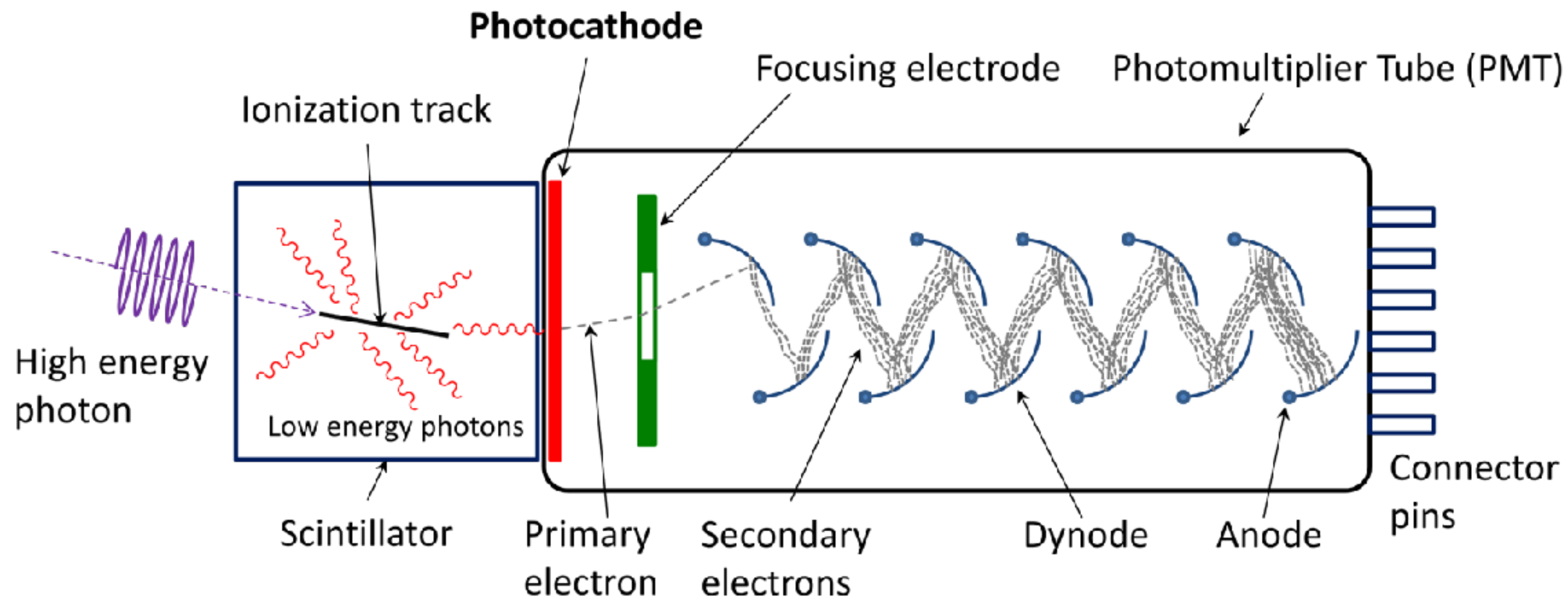
Special aspects of photon detection

This ‘ordinary’ Compton process is taken advantage of for photon detection. In **astrophysical sources the inverse Compton scattering** is important. In such a process a **low-energy photon might gain substantial energy in a collision with an energetic electron**, and it can be shifted into the X-ray or γ -ray domain.

b) Compton scattering:



Photomultiplier



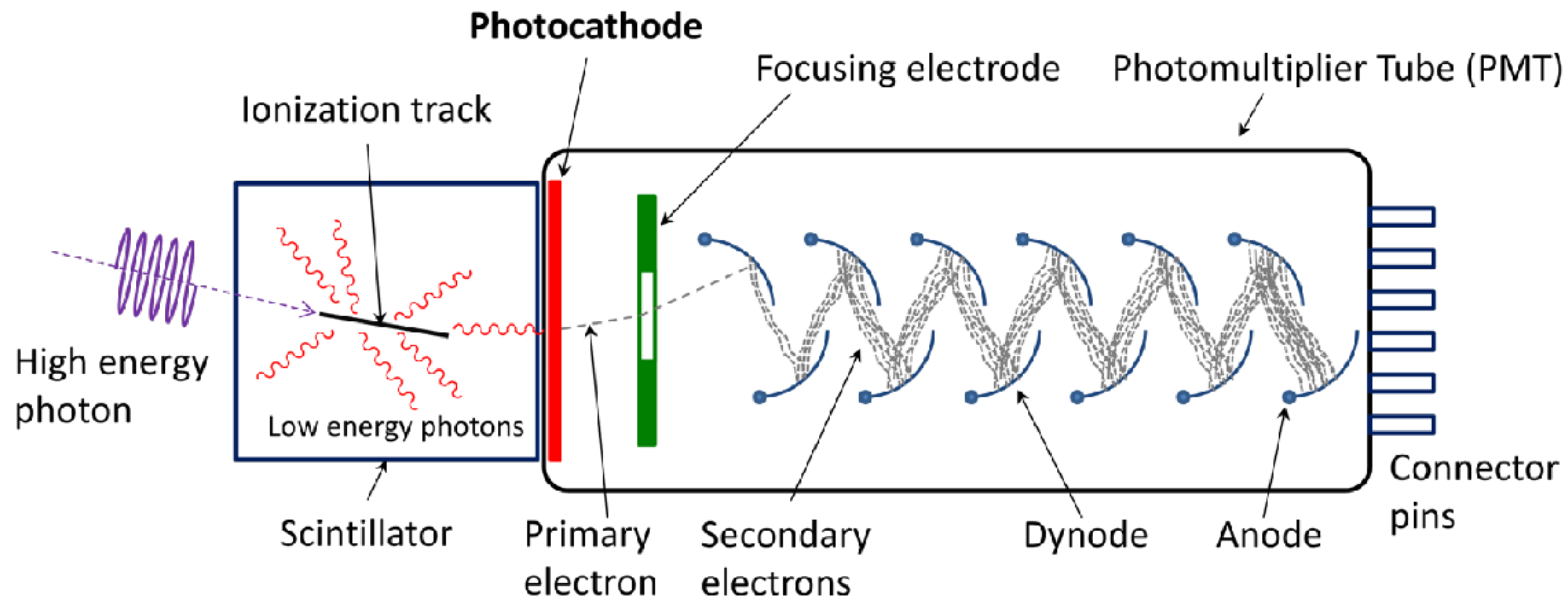
Schematic of a photomultiplier tube coupled to a scintillator. This arrangement is for detection of gamma rays.

Photomultiplier tubes (photomultipliers or PMTs) **are extremely sensitive detectors of light in the ultraviolet, visible, and near-infrared ranges of the electromagnetic spectrum**. These detectors multiply the current produced by incident light by as much as 100 million times (10^8), in multiple dynode stages, enabling (for example) **individual photons to be detected** when the incident flux of light is low.



Photomultiplier

Photomultiplier



Schematic of a photomultiplier tube coupled to a scintillator. This arrangement is for detection of gamma rays.



Dynodes inside a Photomultiplier

Scintillation

Scintillation is the physical process where a material, called a scintillator, emits ultraviolet or visible light under excitation from high energy photons (X-rays or gamma rays) or energetic particles (such as electrons, alpha particles, neutrons, or ions).



Various scintillation crystals. The second crystal from the left is targeted by an UV source and shines brightly in visible light.

Special aspects of photon detection

At high photon energies, the process of **electron–positron pair creation dominates**.

Similarly to Compton telescopes, the **electron and positron tracks** enable the direction of the incident photon to be determined. The photon energy is obtained from the sum of the electron and positron energy. This is normally determined in **electromagnetic calorimeters**, in which electrons and positrons deposit their energy to the detector medium in alternating bremsstrahlung and pair-production processes. These electromagnetic calorimeters can be **total-absorption crystal detectors** such as NaI or CsI, or they can be constructed along the so-called **sandwich principle**.

A sandwich calorimeter is a system, where **absorber and detector layers alternate**. Particle multiplication occurs preferentially in the passive absorber sheets, whilst the shower of particles produced is recorded in the active detector layers. Sandwich calorimeters can be compactly constructed and highly segmented, however, they are inferior to crystal calorimeters as far as the energy resolution is concerned.

Calorimeters

One of the most important and powerful detector techniques in experimental particle physics

Two main categories of Calorimeter:

- **Electromagnetic calorimeters** (interaction through the EM force) for the detection of e^\pm and neutral particles γ
- **Hadron calorimeters** (interaction through the strong) for the detection of π^\pm, p^\pm, K^\pm and neutral particles n, K_L^0
 μ^\pm usually traverse the calorimeters losing small amounts of energy by ionisation
- The 13 particle types above completely dominate the particles from high energy collisions reaching and interacting with the calorimeters
- All other particles decay ~instantly, or in flight, usually within a few hundred microns from the collision, into one or more of the particles above

Neutrinos, \rightarrow can be inferred from measurements of missing transverse energy in collider experiments

Calorimeters

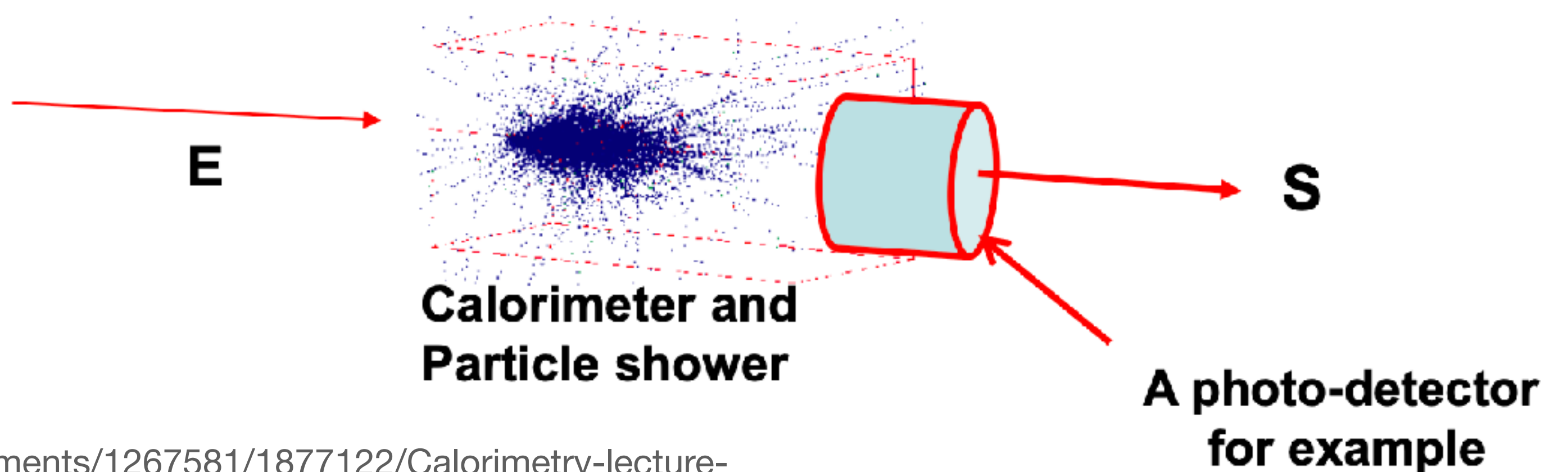
Calorimeters designed to stop and fully contain their respective particles

Measure:

- energy of incoming particle(s) by total absorption in the calorimeter
- spatial location of the energy deposit
- (sometimes) direction of the incoming particle

Convert energy E of the incident particle into a detector response S

Detector response: $S \propto E$



Calorimeters

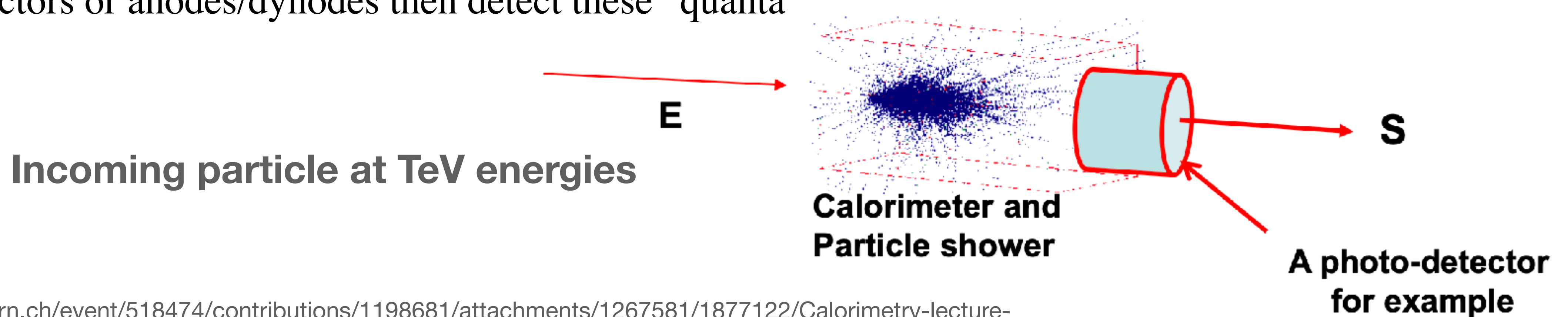
Calorimeter basic mechanism:

Energy lost by the formation of **electromagnetic** or **hadronic** cascades /showers in the material of the calorimeter → Many charged particles in the shower → The charged particles ionize or excite the calorimeter medium

The ionisation or excitation can give rise to:

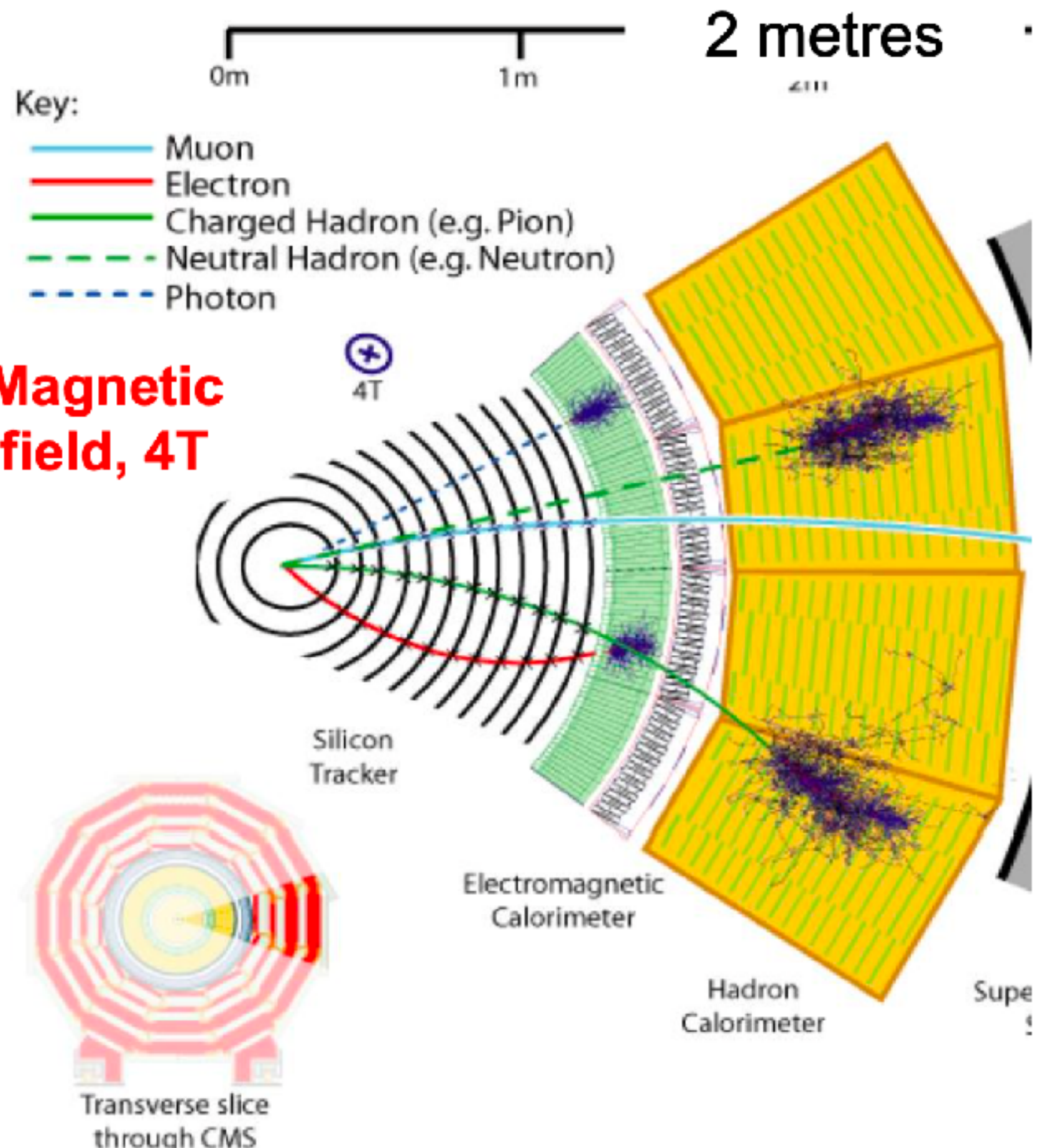
- The emission of visible photons, (eV), via scintillation
- The release of ionisation electrons, (eV)

Photo-detectors or anodes/dynodes then detect these “quanta”

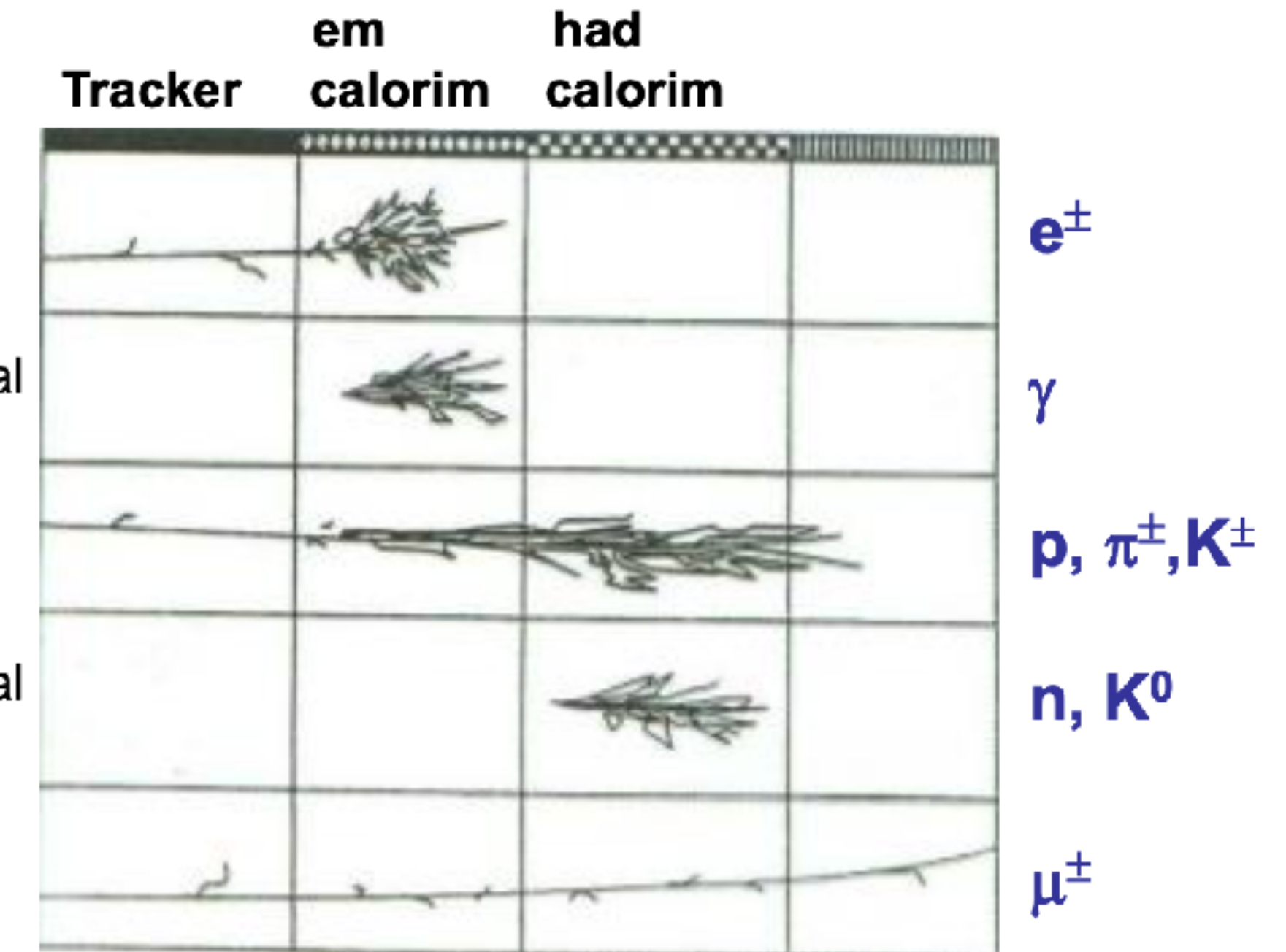


Calorimeters

Where you STOP is what you ARE !!!



A 'wedge' end on view of the CMS experiment at the LHC



Get sign of charged particles from the Tracker

Tracker to be of minimum material to avoid losing particle energy before the calorimeters.

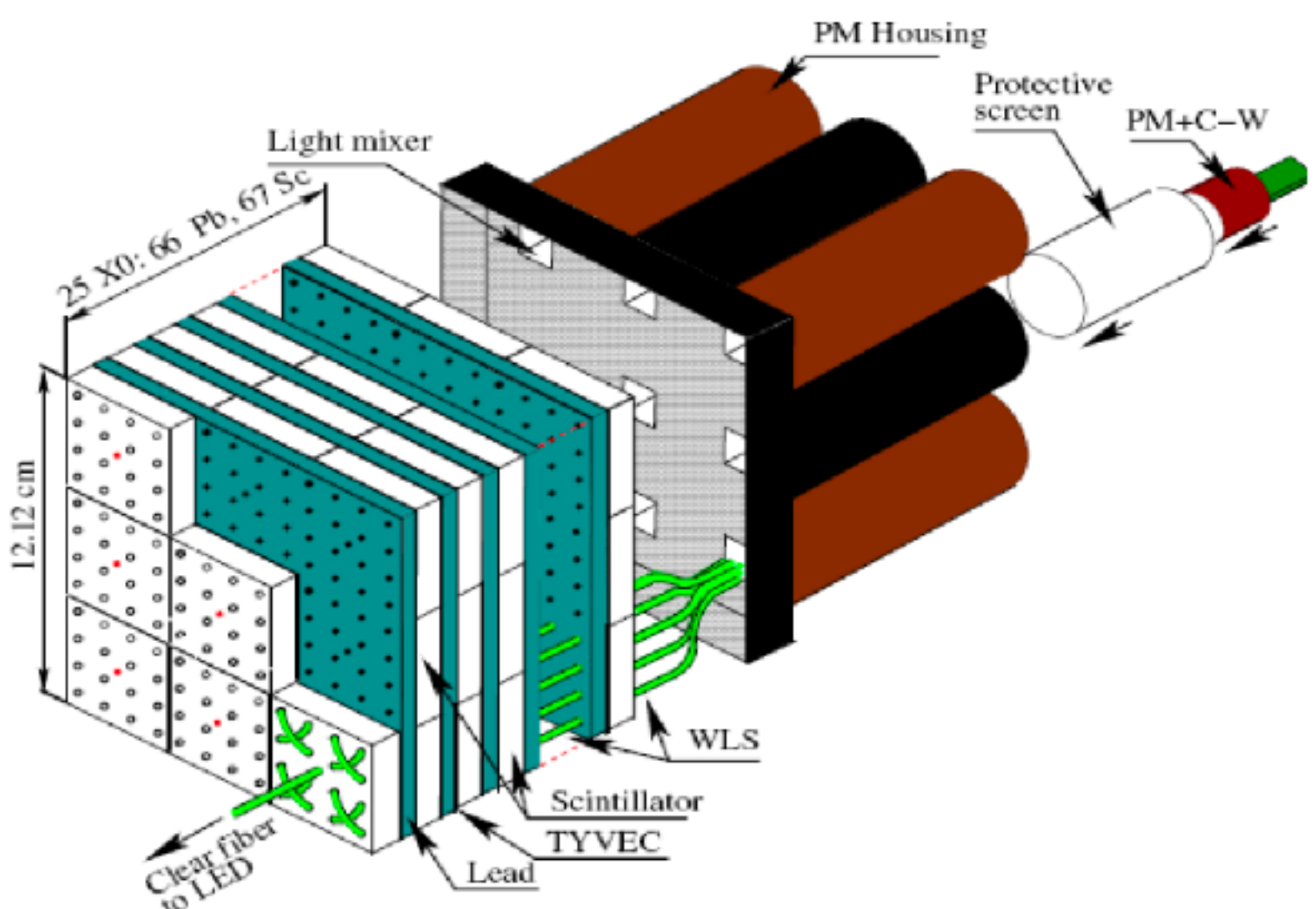
Calorimeters

There are two general types of calorimeter design:

1) Sampling calorimeters

Layers of passive absorber (ie Pb or Cu) alternating with active detector layers such as plastic scintillator, liquid argon or silicon

- Only part of the energy is sampled
- Used for both electromagnetic and hadron calorimetry
- Cost effective



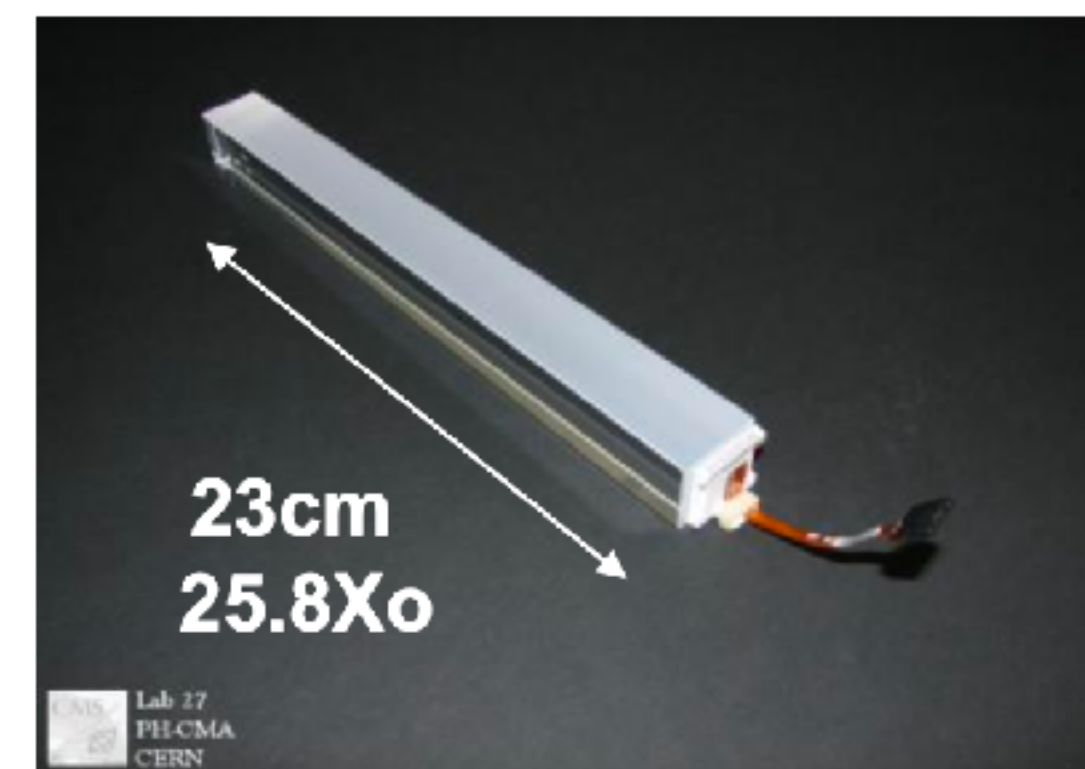
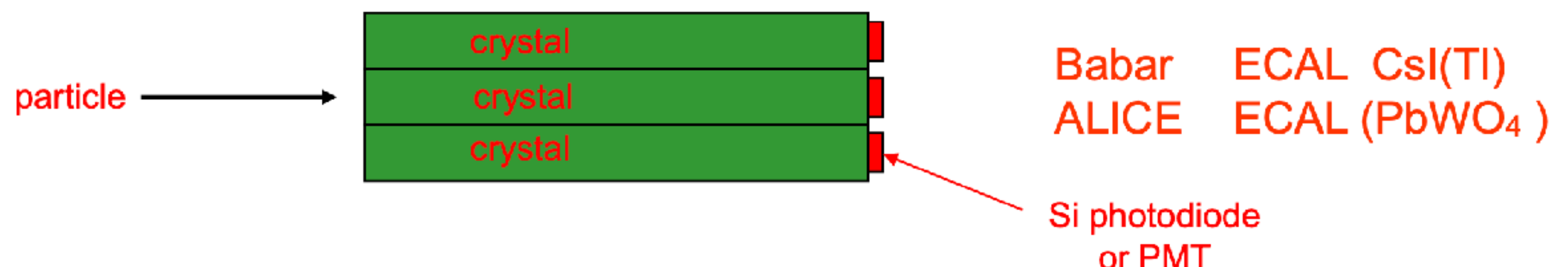
Calorimeters

2) Homogeneous calorimeters

Single medium, both absorber and detector

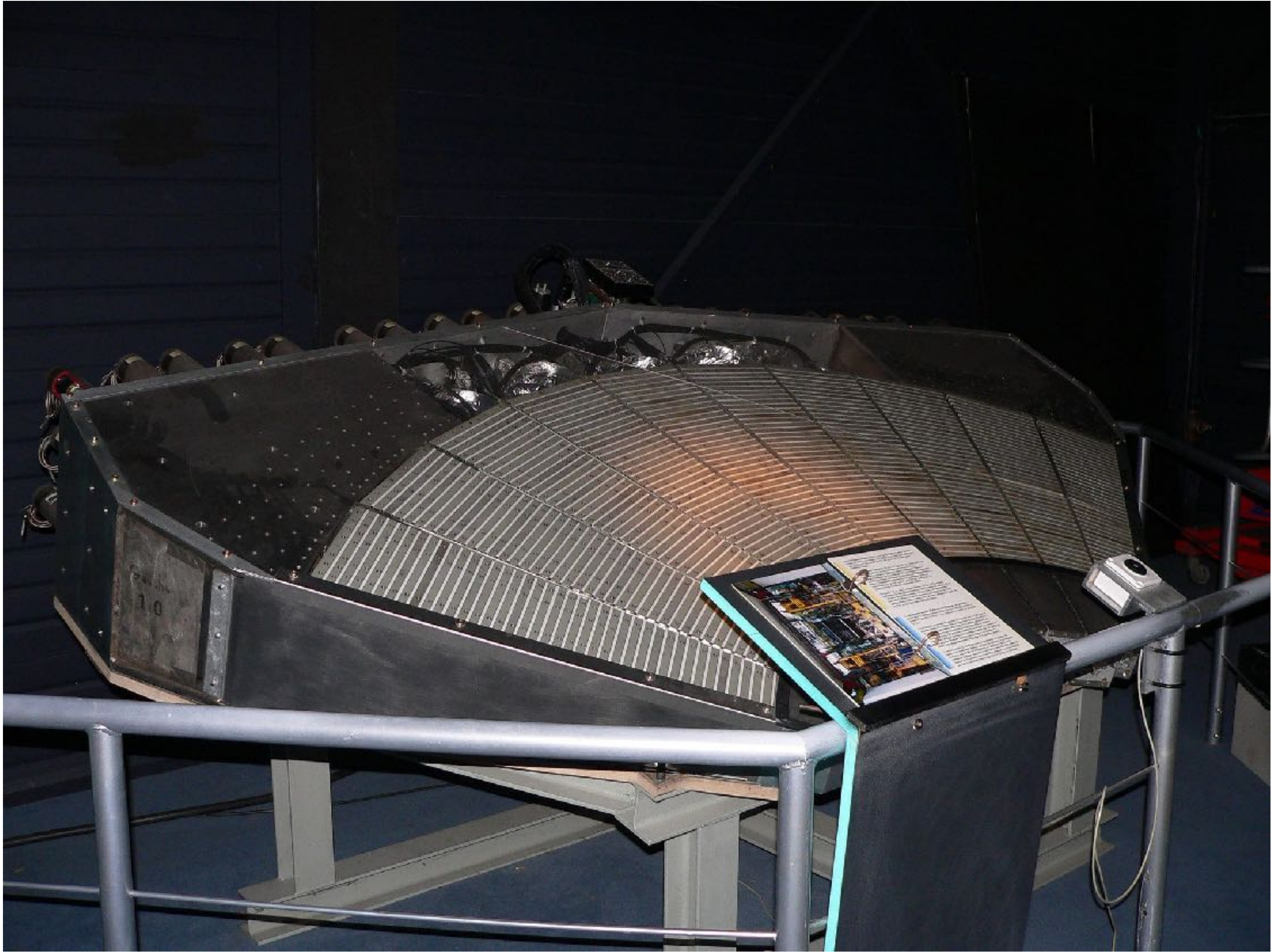
- Liquified Ar/Xe/Kr
- Organic liquid scintillators, large volumes, Kamland, Borexino, Daya Bay
- Dense crystal scintillators: **PbWO₄**, CsI(Tl), BGO and many others
- Lead loaded glass

Almost entirely for electromagnetic calorimetry



CMS ECAL (PbWO₄)

Calorimeters



a Calorimeter in CERN